Universidade de Aveiro Departamento de Ciências Médicas
Ano 2018

Francisco José Furtado Santos

Estudo do metaboloma de linhas celulares de cancro da próstata por FTIR

Studying prostate cancer cell lines metabolome with FTIR spectroscopy

Universidade de Aveiro Departamento de Ciências Médicas
Ano 2018

Francisco José Furtado Santos

Estudo do metaboloma de linhas celulares de cancro da próstata por FTIR

Studying prostate cancer cell lines metabolome with FTIR spectroscopy

Dissertação apresentada à Universidade de Aveiro para cumprimento dos requisitos necessários à obtenção do grau de Mestre em Biomedicina Molecular, realizada sob a orientação científica da Doutora Carla Alexandra Pina da Cruz, Professora Auxiliar Convidada do Departamento de Ciências Médicas da Universidade de Aveiro, e coorientação científica da Doutora Margarida Sâncio da Cruz Fardilha, Professora Auxiliar com Agregação do Departamento de Ciências Médicas da Universidade de Aveiro.

This work was financed by national funds through FCT–Foundation for Science and Technology, under the projects POCI-01-0145-FEDER-016728 and PTDC/DTP-DES/6077/2014, and UID/BIM/04501/2013 and POCI-01-0145-FEDER-007628.

o júri

presidente

Prof. Doutora Ana Gabriela da Silva Cavaleiro Henriques
professora Auxiliar Convidada do Departamento de Ciências Médicas da Universidade de Aveiro

Prof. Doutora Rita Maria Pinho Ferreira
professora Auxiliar do Departamento de Química da Universidade de Aveiro

Prof. Doutora Carla Alexandra Pina da Cruz Nunes
professora Auxiliar Convidada do Departamento de Ciências Médicas da Universidade de Aveiro

agradecimentos

Um agradecimento especial à Prof. Doutora Alexandra Nunes, por toda a disponibilidade e por confiar no meu trabalho. Muito obrigado pelo apoio, rigor e excelente orientação.

À Prof. Doutora Margarida Fardilha, obrigado pelo apoio, disponibilidade e por me integrar na sua equipa.

À Sandra Magalhães, muito obrigado por toda a ajuda que me deste durante a realização da minha dissertação.

Às meninas do Signal Transduction Lab, obrigado pela ajuda, pelo apoio e, sobretudo, pela amizade.

Àqueles que sempre acreditaram em mim. À minha família, obrigado pelo amor e pela força. Aos meus amigos, obrigado pela ajuda e força, sem vocês nunca teria conseguido. Ao José Pedro, obrigado pelo apoio, preocupação e paciência.

Por último, agradeço à minha mãe. Obrigado por todo o amor e confiança que depositas em mim. Agradeço-te por me ensinares a ser uma pessoa trabalhadora, responsável e que luta pelos seus objetivos.

palavras-chave

Cancro da próstata, linhas celulares, metabolómica, perfil metabólico, espectroscopia de FTIR, análise multivariada

resumo

O cancro é uma das principais causas de morte no mundo, sendo o cancro da próstata o segundo mais comum nos homens. Por isso, o desenvolvimento de estratégias que possam fornecer um diagnóstico precoce é de extrema relevância. Uma vez que as alterações bioquímicas precedem as modificações morfológicas nas células, o estudo do metaboloma do cancro tem ganhado relevância e poderá contribuir para a compreensão da biologia do cancro e identificação de biomarcadores de diagnóstico precoce.

A espectroscopia de infravermelho, em particular por FTIR, é uma técnica de metabolómica que, ao contrário de procedimentos histopatológicos, é rápida, não destrutiva e não requer o uso de reagentes. Esta técnica é capaz de detetar a composição bioquímica das amostras e permite a distinção de amostras com perfis metabólicos distintos, possibilitando, assim, a discriminação de células tumorais e normais.

Os principais objetivos deste estudo foram explorar a capacidade do FTIR, acoplado a análise multivariada, na: (1) discriminação entre células de tumor primário de próstata (22Rv1) e células epiteliais normais (PNT1A e PNT2); e (2) discriminação entre células de tumor primário e células provenientes de metástases (LNCaP, de nódulo linfático, e PC-3, de osso).

Através da análise por PCA observou-se uma discriminação entre as diferentes linhas celulares, sugerindo que possuem diferentes perfis metabólicos. A separação entre as diferentes células pode ser atribuída a alterações no metabolismo lipídico (3000-2800 cm^{-1}, 1800-1700 cm^{-1} and 1500-1400 cm^{-1}) e à presença de agregados proteicos (1622 cm^{-1}).

Os nossos resultados sugerem que o estudo do metaboloma do cancro, por FTIR, não só permite a compreensão da patogénese tumoral, como também poderá contribuir para a identificação de biomarcadores de diagnóstico precoce, que são importantes para um bom prognóstico.

keywords

Prostate cancer, cell lines, metabolomics, metabolic profile, FTIR spectroscopy, multivariate analysis

abstract

Cancer is one of the leading causes of death worldwide, with prostate cancer being the second most common neoplasia amongst men. Thus, strategies that can provide an early diagnosis of this disease are of great importance. Because biochemical alterations precede morphological changes in cells, cancer metabolome has gained relevance and may contribute to the understanding of tumor biology and to the identification of early diagnostic biomarkers.

Fourier-transform infrared (FTIR) spectroscopy is a metabolomics technique that, unlike staining procedures and other histopathologic approaches, is rapid, non-destructive and does not require reagents. This technique probes the biochemical composition of the analyzed samples and allows the discrimination of samples with distinct metabolic profiles, thus discriminating cancerous and non-cancerous samples.

The main goals of this work were to explore the ability of FTIR spectroscopy, coupled with multivariate analysis, in the: (1) discrimination between prostate cancer cells derived from a primary tumor (22Rv1) and normal epithelial cells (PNT1A and PNT2); and (2) discrimination between prostate primary tumor cells (22Rv1) from metastatic cells derived from two distinct sites (LNCaP, from lymph node, and PC-3, from bone).

A clear discrimination between the different prostate cell lines was observed, indicating that they exhibit different metabolic profiles. This discrimination can be attributed to an altered lipid metabolism (3000-2800 cm^{-1}, 1800-1700 cm^{-1} and 1500-1400 cm^{-1}) and the presence of protein aggregates (1622 cm^{-1}).

Our results suggest that studying cancer metabolome with FTIR spectroscopy not only allows the understanding of tumor pathogenesis, but also may be a valuable tool for the identification of early diagnostic biomarkers, which are crucial for a good prognosis.

List of publications

- Santos F, Magalhães S, Henriques MC, Fardilha M, Nunes A. Spectroscopic features of cancer cells: FTIR spectroscopy as a tool for early diagnosis. Current Metabolomics. 2018; 6, 103-111.
- Santos F, Magalhães S, Henriques MC, Silva B, Valença I, Ribeiro D, Fardilha M and Nunes A. Understanding prostate cancer cells metabolome: a spectroscopic approach. Submitted to Spectrochimica Acta Part A: Molecular and Biomolecular Spectroscopy on July 17th, 2018.

Poster Communications

- Santos F, Magalhães S, Henriques MC, Silva B, Valença I, Ribeiro D, Fardilha M and Nunes A. Discrimination between tumoral and normal prostate cells by FTIR spectroscopy. Conference: Jornadas do CICECO 2018. June 2018.
- Santos F, Magalhães S, Henriques MC, Silva B, Valença I, Ribeiro D, Fardilha M and Nunes A. Understanding prostate cancer cells metabolome: a spectroscopic approach. Congress: I NoTeS Congress - Novel Therapeutic Strategies for Noncommunicable Diseases. June 2018.
- Santos F, Magalhães S, Henriques MC, Silva B, Valença I, Ribeiro D, Fardilha M and Nunes A. Discrimination between prostate cancer and normal prostate cell lines by FTIR spectroscopy. Symposium: IV Postgrad Symposium in Biomedicine. July 2018.

This dissertation is organized in parts A, B and C

A. General Introduction and Aims, includes:

- Published review article

  Santos F, Magalhães S, Henriques MC, Fardilha M, Nunes A. Spectroscopic features of cancer cells: FTIR spectroscopy as a tool for early diagnosis. Current Metabolomics. 2018; 6, 103-111.

B. Results, includes

- Submitted research article

  Santos F, Magalhães S, Henriques MC, Silva B, Valença I, Ribeiro D, Fardilha M and Nunes A. Understanding prostate cancer cells metabolome: a spectroscopic approach. Submitted to Spectrochimica Acta Part A: Molecular and Biomolecular Spectroscopy.

C. Concluding remarks, limitations and future perspectives

Table of contents

Table of Figures

Table of Tables

List of Abbreviations

ATR	Attenuated total reflectance
BPH	Benign prostatic hyperplasia
FTIR	Fourier-transform infrared spectroscopy
IR	Infrared
NMR	Nuclear magnetic resonance
PBS	Phosphate-buffered saline
PC	Principal component
PCA	Principal component analysis
PLS-DA	Partial least square – discriminant analysis
PCa	Prostate cancer
PSA	Prostate-specific antigen
TIR	Total internal reflection

A. General Introduction and Aims

1. Spectroscopic features of cancer cells: FTIR spectroscopy as a tool for early diagnosis

Francisco Santos[a,b], Sandra Magalhães[a], Magda Carvalho Henriques[b], Margarida Fardilha[b] and Alexandra Nunes[a]

[a] iBiMED – Institute of Biomedicine, Department of Medical Sciences, University of Aveiro, Aveiro, Portugal

[b] Signal Transduction Laboratory, iBiMED – Institute of Biomedicine, Department of Medical Sciences, University of Aveiro, Aveiro, Portugal

Corresponding author: Alexandra Nunes, iBiMED – Institute of Biomedicine, Department of Medical Sciences, University of Aveiro, Agra do Crasto, 3810-193, Aveiro, Portugal. E-mail: alexandranunes@ua.pt

1.1 Abstract

Globally, cancer is one of the leading causes of death, so the development of strategies for an early diagnosis of cancer is of great importance. Biochemical alterations precede morphological changes in cells and tissues, so studying cancer metabolome seems like a reasonable approach for early diagnosis, prognosis and to follow treatment progression. Fourier-transform infrared (FTIR) spectroscopy is a valuable tool for studying the metabolome of biological samples, such as cancer cell lines. Unlike staining procedures and other histopathologic approaches, this technique is rapid, non-destructive and does not require reagents. The spectral differences that result from probing the biochemical composition of cancer and normal cells are indicative of distinct metabolic profiles, which allow the discrimination of different cells. Using FTIR spectroscopy and multivariate statistical analysis, several alterations concerning the content of lipids, proteins, nucleic acids and carbohydrates have been identified in cancer cells, some of which can be regarded as potential biomarkers. This review focuses on FTIR spectroscopy as a metabolomics tool to study and characterize cancer cell lines.

1.2 Introduction

Cancer is the second leading cause of death worldwide. It is estimated that there are 14 million new cases of the disease every year, causing almost 9 million deaths (1,2). Despite the efforts in finding new diagnostic and therapeutic strategies, cancer patients exhibit relatively low survival rates. One of the reasons for that is the fact that the disease is often detected when it is well established, meaning that it is diagnosed at a late stage, only when morphological alterations are observed, in many cases resulting in a poor prognosis (3). Furthermore, costs associated with cancer treatment are a huge problem for healthcare systems, so it is imperative to discover new strategies to diagnose cancer as early as possible (4,5).

Similar to every other disease, cancer exhibits several cellular and molecular alterations (6–8). Because cancer cells display a very distinct and unique metabolic phenotype, cancer is basically considered a metabolic disease. Moreover, an altered metabolism has been recognized as one of the hallmarks of cancer (9,10). Since it is the endpoint of cellular biological processes, metabolism carries an imprint of the cell's phenotype and, therefore, is indicative of its activity. Common alterations present in several types of cancer cells include increased glucose uptake, increased rate of glycolysis, decreased

mitochondrial activity, low bioenergetic status and abnormal phospholipid metabolism (11–13). In addition to these general metabolic alterations, specific metabolites have been implicated in particular types of cancer, such as 1-stearoylglycerol, citrate and spermine in prostate cancer (14,15) and glycine in breast cancer (16). Thus, measuring metabolites themselves appears to be a reasonable approach to study diseased cells (17).

The study of the metabolome provides rapid, sensitive and reproducible data and has been widely used to understand phenotypic and metabolic alterations associated with cancer cells (18–20). The main advantage of metabolomics lies on the fact that the metabolome can reflect early changes that occur in the cell, allowing the identification of diagnostic biomarkers before morphological changes occur (18,21). Furthermore, metabolomics allows to monitor the efficacy of medical interventions and the understanding of molecular mechanisms involved in cancer and carcinogenesis (21,22).

The main metabolomic techniques used for metabolic fingerprinting are nuclear magnetic resonance (NMR) spectroscopy, mass spectrometry and vibrational spectroscopy, which includes FTIR spectroscopy (17,23). The latter has gained relevance in biomedical research because it provides an inexpensive, rapid, high-throughput and non-destructive analysis of a wide range of samples, including biological fluids, tissues and cells (24,25). FTIR spectroscopy probes the chemical composition and molecular structure of the analyzed samples (17,26). Moreover, since biochemical alterations lead to spectral differences, it is possible to discriminate samples with distinct metabolic profiles (3,27). In this review, we intend to explore the importance of FTIR spectroscopy in cancer metabolomics and compile work that has been conducted in the study of cancer cell lines using FTIR spectroscopy.

1.3 FTIR Spectroscopy

FTIR spectroscopy is a form of vibrational spectroscopy. Therefore, it is based on the vibrations of the atoms in a molecule, caused by the interaction of infrared (IR) radiation with matter (28–30). However, not every molecule shows IR absorptions: only the vibrations that cause a change in the dipole moment of the molecule absorb IR radiation, and the larger this change, the more intense the absorption band will be (29). Molecular vibrations that are produced (mainly stretching and bending) are specific to the composition and structure of analyzed samples (24,26,29). The IR region can be divided into three regions: near-IR (13,000 – 4,000 cm^{-1}), mid-IR (4,000 – 400 cm^{-1}) and far-IR (< 400 cm^{-1}) (29). Nevertheless, many of the studies that have been conducted regarding

FTIR spectroscopy and cell lines included only the mid-IR region because, aside from being very informative, most of the molecules absorb its radiation (31,32).

FTIR spectroscopy has shown potential as a tool for analyzing cells. Unlike histopathologic techniques, FTIR spectroscopy is rapid, non-invasive, cost-effective, easy to operate, reagent-free and requires minimal sample preparation. Furthermore, experimental materials can be re-used for further analysis and, as it is a method without technician interference, it tends to be less subjective (17,25,30). Despite these great advantages, one of the main disadvantages of this technique is the strong absorption that water exhibits in the mid-IR region. As biological tissues and cells are mainly composed by water, this may constitute a problem in FTIR analysis of biological samples. Nevertheless, this drawback can be overcome simply by dehydrating the samples, ridding them of the water (17,33–35).

Since IR spectra reflect the chemical composition of a given sample, alterations that occur in key macromolecules, such as proteins, lipids, carbohydrates and nucleic acids, can be monitored (36–39). Furthermore, IR spectrum can be considered a molecular fingerprint of the sample, meaning that changes that occur in biomolecules, for instance, during carcinogenesis, will modify this fingerprint, enabling the discrimination between cancer and normal cells (37,40–42).

To analyze FTIR data, both direct spectra analysis and statistical tools can be used. In spite of its importance, direct analysis of IR spectra is difficult and subjective, so multivariate statistical tools are widely used instead to study metabolomics data (43,44). One of the most commonly used tools is principal component analysis (PCA), which is an unsupervised model, so it does not require an initial knowledge about the samples (43,45). PCA reduces thousands of variables characteristic of a spectrum to a few principal components and is used as an exploratory tool that groups samples according to shared similarities (43,46). The results of a PCA can be presented in the form of score and loadings plots; score plots present the separation of groups observed in the samples, while loadings plots indicate variables that are responsible for the discrimination (44,46). After the samples are analyzed with an unsupervised model, other statistical methods can be applied, such as partial least square – discriminant analysis (PLS-DA). This is a supervised model, meaning that an initial knowledge about the samples is required (e.g. cancer cells vs. normal cells) and can be used if the discrimination provided by PCA is insufficient (43,44,47). After the use of appropriate multivariate analysis tools, it is possible

to create quantitative and qualitative classification models that make analysis of spectroscopic data more objective and, in some cases, almost automatic.

1.4 Cell lines for *in vitro* study of cancer

Cells are composed by several macromolecules, such as proteins, lipids, nucleic acids and carbohydrates (24). Therefore, the study of cells can provide a great deal of information regarding metabolic processes and absence or presence of disease (48).
Human cancer-derived cell lines are considered an important asset in biomedical research among the other tools of studying cancer. Since they offer an almost unlimited source of cells, are relatively easy to work with, exhibit a high degree of homogeneity and provide consistent and reproducible results, cancer cell lines have become the most used experimental model to study cancer. Furthermore, the use of cancer cell lines evades ethical issues that are associated with the use of animal and human tissues (49,50).

Cancer cell lines are widely used to study the biology of cancer and in the development and testing of anticancer drugs, and many of the results that are obtained with cell lines are extrapolated to human cancers *in vivo* (51–55). The most commonly used approaches for the study of cells rely on staining procedures, which can be expensive, time-consuming and potentially cause harmful effects on the cells (56). Therefore, new approaches to study cell lines, such as FTIR spectroscopy, have emerged in the last years, showing promising results (36,41,57).

1.5 FTIR spectroscopy applied to cancer cell lines

FTIR spectroscopy has proven to be a valuable tool in cancer metabolomics. When analyzing biological samples, such as cells, there are key spectral regions that need to be considered. The 3000 – 2800 cm^{-1} region is mainly associated to lipids. Proteins are mostly characterized by two bands in the 1800 – 1300 cm^{-1} region: amide I, between 1700 and 1600 cm^{-1}, and amide II, which peaks at ~1540 cm^{-1}, which are sensitive to the secondary structure of proteins; however, the amide I band is the most frequently used for this type of analysis. Also, in the 1800 – 1300 cm^{-1} region, the shoulder band at ~1740 cm^{-1} is assigned to phospholipids, and the bands between 1480 and 1300 cm^{-1} have been attributed to amino acid side chains and fatty acids. Lastly, the major bands in the 1300 – 900 cm^{-1} region arise mainly due to carbohydrates (particularly glycogen) and phosphates associated with nucleic acids (17,58). Furthermore, any changes in intensity or shape of bands or shifts to lower or higher frequencies, may indicate cellular alterations (58). A

more detailed description of the mid-IR bands and their assignments can be consulted in table 1.

Table A.1: Major vibrational modes and corresponding assignments found in biological samples.

Wavenumber (cm^{-1})	Vibrational mode	Assigned biochemical component	Reference
~3300	N-H stretching	Amide A: peptide, protein	(28,83)
~3100	N-H stretching	Amide B: peptide, protein	(28,83)
~2960	CH_3 asymmetric stretching	Lipids	(24,70,71)
~2925	CH_2 asymmetric stretching		
~2870	CH_3 symmetric stretching		
~2853	CH_2 symmetric stretching		
~1740	C=O stretching	Phospholipid esters	(24,48,83)
~1683	C=O stretching, C-N stretching, in-plane N-H bending	Amide I: antiparallel β-sheets	(24,57)
~1650		Amide I: α-helices	(24,57)
~1635		Amide I: parallel β-sheets	(24,57)
~1550 – 1520	N-H stretching, C-N stretching, C-C stretching	Amide II	(24,83)
~1460 – 1400	CH_3 and CH_2 deformation	Membrane lipids and proteins	(67,74,83)
~1380	CH_3 symmetric wagging	Phospholipid, fatty acid, triglyceride	(83)
~1310 – 1200	N-H bending, C-N stretching, C=O stretching, C-C stretching, CH_3 stretching	Amide III	(24,83,84)
~1240	PO_2^- symmetric stretching	Nucleic acids	(27,69)
1170	C-O stretching	Tyrosine, serine and threonine of cell proteins	(67)
1155	C-O stretching, C-O-H bending	Carbohydrates	(67)
1122 – 1120	Vibration mode of the PO_2^- of the phosphodiester groups	RNA	(69,71)
1086 – 1080	PO_2^- symmetric stretching	DNA, RNA, phospholipid, phosphorylated protein	(67,69)
1047, 1025	C–O stretching and bending of C–OH	Glycogen	(67)
972 – 970	PO_3^{2-} symmetric stretching	Dianionic phosphate monoesters of phosphorylated proteins and nucleic acids	(67,70)

1.5.1 Spectral characteristics of cancer cell lines

A typical IR spectrum of cancer cells is presented in figure A.1. The spectrum represents an average of 8 spectra, which were acquired in a Fourier-transform infrared spectrometer (Alpha Platinum ATR, Bruker), controlled by OPUS software (©Bruker). The spectra were obtained over the wavenumber range 4000-600 cm^{-1}, with a resolution of 8 cm^{-1} and 64

co-added scans. The cell suspension was air-dried to remove water and, therefore, prevent its strong absorption. The spectral assignments for the cells were made according to table A.1.

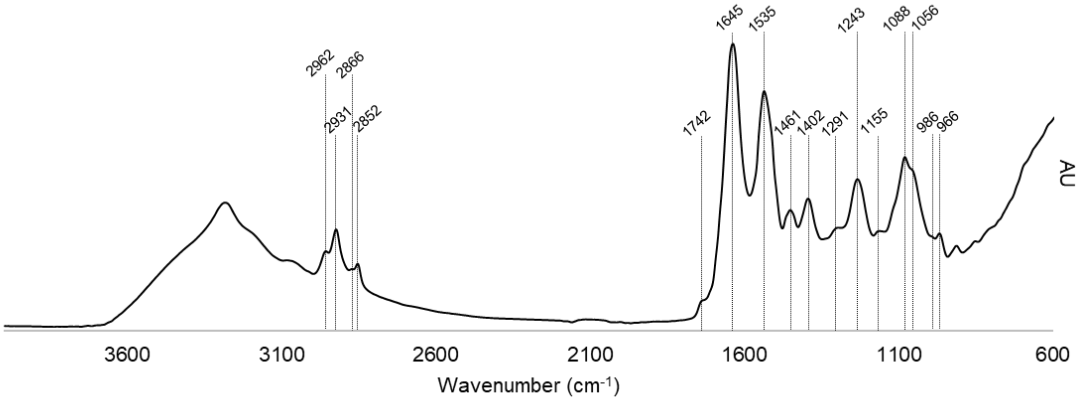

Figure A.1: IR spectrum of prostate cancer cells LNCaP in the 4000-600 cm^{-1} region with the main spectroscopic signals. The spectrum represents the average of 8 spectra. X-axis: wavenumber (cm^{-1}); Y-axis: arbitrary units (AU).

The study of cancer cell lines with FTIR spectroscopy came to light when Rigas and colleagues observed that several colon adenocarcinoma cell lines (LoVo, SW1116, HCT-15, SW403, SW480) had similar spectra to those of colon cancer tissues (59). In a subsequent study, Rigas and Wong compared the same cell lines and an additional adenocarcinoma lineage (SKC01) to normal and malignant colon tissues. They observed that these cells shared many characteristics with malignant colon tissues, such as an increased hydrogen-bonding of the phosphodiester groups of nucleic acids (57). In addition, they observed that the symmetrical PO_2^- stretching causes a band shift from 1082 cm^{-1} (in normal tissue) to 1086 cm^{-1} (in adenocarcinoma cells). In the 1010 – 950 cm^{-1} region, two bands were discovered in adenocarcinoma cell lines: one at 972 cm^{-1}, assigned to nucleic acids and symmetrical stretching mode of dianionic phosphate monoesters of phosphorylated proteins, and the other at 991 cm^{-1}, which varies amongst cell lines and wasn't assigned to any particular biochemical component (57). Previous results obtained with HCT-15 cells also indicated that the phosphodiester stretching bands are related to nucleic acids (60). Lastly, Rigas and Wond studied the amide I band in the 1700 – 1600 cm^{-1} region, assigned to the in-plane C=O stretching vibration weakly coupled with C-N stretching and in-plane N-H bending of the amide groups of proteins. They observed an increase in the relative amount of β-sheets, in relation to α-helical segments, in adenocarcinoma cells and malignant tissue in comparison with normal tissue (57). It is already known that β-sheets are highly present in less soluble proteins that are

likely to form aggregates (61,62). Similar to neurodegenerative diseases, protein aggregation has been found to be present in many types of tumors and cancer cell lines, mainly involving aggregates of the tumor suppressor p53 (63–65), which can play an important role in carcinogenesis and drug resistance (66).

In a study comparing the uterine cervical adenocarcinoma cell line SiSo with cervical adenocarcinoma tissue and exfoliated malignant and normal cervical cells, Neviliappan and colleagues observed that several spectral bands of the malignant tissue and exfoliated cells and the SiSo cell line were noticeably different from those of the normal exfoliated cells (67). The bands at 1047 and 1025 cm^{-1} (usually called glycogen bands) are associated mostly with C-O stretching and bending of the C-OH groups of carbohydrates and were significantly reduced in the malignant tissue and exfoliated cells, and in the SiSo cell line (67). Similarly, the band at 1155 cm^{-1}, assigned to the C-OH stretching mode of carbohydrates, exhibited a lower peak in the abnormal cases due to the decrease of the glycogen levels. A shift in the frequency from 1080 cm^{-1} (in normal cases) to 1085 cm^{-1} (in abnormal cases) was also observed, indicating a strong intermolecular interaction that occurs in nucleic acids, suggesting that DNA packing is tighter and higher in malignant tissue and exfoliated cells and in the SiSo cell line. Also, an increase of intensity of the band at 970 cm^{-1} was observed in the abnormal cases. Furthermore, a peak at 1170 cm^{-1} was detected in malignant tissue, exfoliated cells and SiSo cell line, which is derived from the C-OH groups of tyrosine, serine and threonine of cell proteins, indicating an increase in the phosphorylation of the C-OH groups (67). It has been shown that an increase of the phosphorylation of these three amino acids by oncoproteins is an important event that occurs during carcinogenesis (68). Another shift observed in the spectra of the malignant tissue, exfoliated cells and the SiSo cell line occurred in the band at 1400 cm^{-1}: there was an increase of the intensity of this band in these samples, which might be related to structural changes in the methylene chains of lipids (67).

Later, in 2004, Fujioka and colleagues applied FTIR spectroscopy to compare three gastric cancer cell lines (AGS, SNU-1 and NCI-N87) with normal gastric mucosal epithelial cells (69). In this study, they analyzed the spectral region between 1650 and 925 cm^{-1} and were able to find significant differences between cells, mainly an increase of intensity of bands at 1240, 1120 and 1080 cm^{-1} (69). Regarding the band at 1240 cm^{-1}, a shift to a higher frequency was observed in cancer cells (peak maximum absorbance at ~1241.5 cm^{-1}), compared to the peak maximum absorbance at ~1236.9 cm^{-1} presented by the

normal epithelial cells, suggesting an alteration in the hydrogen bonds in the phosphodiester groups of the DNA in cancer cells. As for the band at 1080 cm^{-1}, authors observed a shift to a higher frequency in two cancer cells (AGS and SNU-1) in comparison to the one detected in normal cells (1085.7 cm^{-1} and 1081.9 cm^{-1}, respectively). This shift can be attributed to the tighter packing of DNA molecules in the cancer cells. On the other hand, a shift to a lower frequency was registered in the NCI-N87 cell line (1081.5 cm^{-1}) (69). Finally, the increased IR absorbance observed in the cell lines in the band at 1120 cm^{-1} was due to an increment of RNA content in these cells. Given these results, the authors concluded that the changes observed in the spectra were all associated with an increase in the phosphate backbone, corresponding to an increase in DNA and RNA content in the cancer cell lines (69).

A few studies using FTIR spectroscopy have also been carried out in breast cancer cell lines. In 2008, Hwang and colleagues studied the 4000-2400 cm^{-1} region to evaluate lipids in cell lines MCF 10A (normal cell line), MCF7 (cancer cell line) and MDA-MB-231 (invasive cancer cell line) (70). They observed major absorption bands at 3683, 3664 3641, 3621, 2923, 2873 and 2854 cm^{-1}, with notable differences at 3621 and 2873 cm^{-1} that were only observed in the MCF 10A cell line. Their results suggest that cancer cells exhibit a stronger bonding structure in the membrane lipids compared to normal cells (70). In 2010, Mostaço-Guidolin and colleagues focused on the study of the MCF7 and SKBr3 cells, which are estrogen receptor positive and negative, respectively (71). Their results indicate that the MCF7 cell line shows increased absorbance intensity in the bands at 1085 (DNA), 1542 (amide II) and 1650 cm^{-1} (amide I), compared to the SKBr3 cell line. Furthermore, differences in the 3000-2800 cm^{-1} region were detected. Their results suggest that SKBr3 cells show an increased IR absorbance in the lipids region, mainly in the bands at 2962 and 2924 cm^{-1} (71).

In the field of lung cancer, Lee and colleagues conducted a study in which they compared two cancer cell lines (NCI-H358 and NCI-H460) to normal human bronchial epithelial (NHBE) cells (72). They observed that the bands at 1085 and 970 cm^{-1} were increased in the cancer cells. These bands are assigned to the symmetric stretching of PO_3^{2-} and PO_2^-, respectively, and the authors attributed this result to an increase of phosphorylation that occurs in cancer cells. Apart from this result, they verified that bands at ~1030 and ~1155 cm^{-1} were more intense in normal cells, suggesting a decrease of glycogen in cancer cells, as was previously reported by Wong and colleagues (72,73).

Hematological cancers have also been subject to IR spectroscopic studies. Babrah *et al.* studied five cell lines derived from human leukemias and lymphomas: Karpas 299 (T-cell lymphoma cell line), REH (acute lymphoid cell line), RCH-ACV (acute lymphoid cell line), *HL60* (acute myeloid leukemia cell line) and Meg01 (chronic myeloid cell line) (74). The results indicated notable changes in the 1500-900 cm^{-1} region, mainly an increase of the intensity of the amide III and DNA bands. This increase might indicate an increment of cellular nuclear content, shedding light on the biochemical differences that exist between the cell lines (74).

In what concerns investigation of drug-resistant cell lines, the band at 1740 cm^{-1} was subject to a couple of studies. Gaigneaux and colleagues were able to determine significant differences in the lipid content between sensitive K562 cells derived from human chronic myelogenous leukemia (K562/DNS) and its multiresistant variant (K562/DNR). A reduction of the intensity of the band in K562/DNR cells suggested a decrease of lipid content (75). Zwielly and colleagues focused on the discrimination of two melanoma cell lines based on their sensitivity to cisplatin: GA (sensitive parental cell line) and GAC (cisplatin-resistant cell line derived from GA). Unlike K562/DNR cells (75), these results indicated an increase of the intensity of the band at 1740 cm^{-1} in the GAC cell line (38). These opposite results can be attributed to the number of passages the cells were subjected to. Le Moyec *et al.* verified that after several passages in the absence of the anticancer drug, K562 cells partially recovered their lipid content (76).

A recent investigation, carried out by Minnes *et al.*, determined that FTIR spectroscopy could also be useful in distinguishing cancer cells with distinct metastatic potentials (77). It has already been proven that metastatic cells exhibit a higher level of fluidity of the cell membrane, which can be associated with a higher level of hydration (78,79). Additionally, an increase in the level of hydration is followed by an increment in the absorption intensity of proteins (80). In this study, two pairs of melanoma cell lines were utilized: murine B16-F1 and B16-F10, and human WM-115 and WM-266.4. It was concluded that cells with a higher metastatic potential (B16-F10 and WM-266.4) exhibited a higher absorption intensity of the band at 1540 cm^{-1} (amide II), in comparison to the cells with a low-metastatic potential (B16-F1 and WM-115), which can be attributed to the higher level of hydration of the cell membrane (77). To sum up all these results, table A.2 presents the main spectral characteristics of cancer cell lines.

Table A.2: Specific spectral characteristics for cancer cell lines.

Mid-IR region	IR frequency	Alterations in the IR spectra
3000 – 2800 cm^{-1}	2962 cm^{-1}	Increased intensity in SKBr3
	2924 cm^{-1}	
	2873 cm^{-1}	Increased intensity in MCF 10A
	2852 cm^{-1}	Increased intensity in GAC
1800 – 1300 cm^{-1}	1740 cm^{-1}	Decreased intensity in K562/DNR
	1700 – 1600 cm^{-1}	Increased number of β-sheets in LoVo, SW1116, HCT-15, SW403, SW480 and SKC01
	1650 cm^{-1}	Increased intensity in MCF7
	1542 – 1540 cm^{-1}	Increased intensity in B16-F1, WM-115 and MCF7
	1400 cm^{-1}	Shift in the spectrum of SiSo
1300 – 900 cm^{-1}	1242 cm^{-1}	Increased intensity in Karpas 299, REH, RCH-ACV, HL60 and Meg01
	1240 cm^{-1}	Shift in the frequency in AGS, SNU-1 and NCI-N87
	1170 cm^{-1}	Increased intensity in SiSo
	1155 cm^{-1}	Decreased intensity in SiSo
	1120 cm^{-1}	Increased intensity in AGS, SNU-1 and NCI-N87
	~1086 – 1080cm^{-1}	Shift in the frequency in LoVo, SW1116, HCT-15, SW403, SW480, SKC01, SiSo, AGS, SNU-1 and NCI-N87 Increased intensity in NCI-H358, NCI-H460 and MCF7
	1047 cm^{-1} and 1030 - 1025 cm^{-1}	Decreased intensity in SiSo, NCI-H358 and NCI-H460
	991 cm^{-1}	Present in LoVo, SW1116, HCT-15, SW403, SW480 and SKC01
	972 – 970 cm^{-1}	Increased intensity in LoVo, SW1116, HCT-15, SW403, SW480, SKC01, SiSo, NCI-H358 and NCI-H460

1.5.2 Potential spectral biomarkers

Apart from the spectral differences between different cancer cells, ratios between specific mid-IR bands have been regarded as potential biomarkers. Gazi *et al.* explored the peak area ratio of 1030 cm^{-1}/1080 cm^{-1}, which corresponds to the glycogen/phosphate ratio, as a potential diagnostic biomarker (36). This ratio correlates with the metabolic turnover of cells, and lower values are observed in malignant cell lines. However, non-malignant cell line PNT2-C2 also exhibits a low ratio, which the authors attributed to the transformation process that cells had to undergo in order to become immortal (36).

In a study comparing two K562 cell lines (75), a decrease of the lipid/protein and nucleic acid/protein ratios, in the 3000-2800 cm^{-1} and 1300-900 cm^{-1} regions, respectively, was detected in the K562/DNR cells. However, a higher 2871 cm^{-1}/2853 cm^{-1} ratio was observed in K562/DNR cells, which can be attributed either to the decrease of lipid content in resistant cells or to the modification of the membrane composition (75). Characteristic IR absorptions were also found at the bands at 2958 cm^{-1} (methyl groups of

lipids and proteins) and 2852 cm^{-1} (methylene chains in membrane lipids) in GA and GAC cells, and the ratio between these two frequencies was considered a potential biomarker to distinguish the two types of cells, with a lower ratio observed in resistant cells (38). Furthermore, lipid/protein ratios using the intensities at 1740 and 1400 cm^{-1} were assessed, and a noteworthy increase of the ratio in resistant cells was detected. The increase of the intensity of the bands at 2852 and 1740 cm^{-1} can be used to monitor lipids in resistant cells and, therefore, is considered a diagnostic parameter that can be associated with drug resistance (38). Also, another potential biomarker was found in the 1200-1000 cm^{-1} region, which was associated to the ratio between RNA (1121 cm^{-1}) and DNA (1022 cm^{-1}). It was found that, in resistant cells, this ratio was higher compared to normal cells (38).

1.5.3 Multivariate analysis applied to FTIR spectra of cancer cell lines

Besides direct spectra analysis, multivariate statistical analysis is a powerful tool to analyze FTIR spectra and has gained an important role in the discrimination of several cell lines (36,41). Wood *et al.* carried out a study in which they compared HeLa cells (derived from cervical cancer) to normal and malignant exfoliated cells (81). Using PCA a clear separation was observed between normal and malignant exfoliated cells. Furthermore, HeLa cells were grouped with the malignant cells, validating the spectral similarities between HeLa and malignant exfoliated cells (81).

In 2003, Gazi and colleagues were able to discriminate, for the first time, prostate cancer cell lines derived from distinct metastatic sites based on their IR spectra (36). Using PCA, they discriminated three cell lines used as models for prostate cancer: DU 145 (derived from brain metastasis), PC-3 (derived from bone metastasis) and non-malignant PNT2-C2 (normal prostate epithelial cells transformed with the genome of SV40 virus to express the large T antigen) (36). In 2009, Harvey and colleagues carried out a similar study, in which they also compared prostate cancer cell lines: PC-3, PNT2-C2 and LNCaP, which is derived from lymph node metastasis. Using the spectral region between 1481-800 cm^{-1}, they were able to discriminate the cells based on their spectra and discard possible factors that could have influenced the discrimination of the prostate cell lines reported by Gazi *et al.* (41). To do so, they studied the effect of the growth media and the nucleus/cytoplasm ratio on this discrimination and verified that neither were able to explain it. Therefore, they concluded that the intrinsic biochemical differences between the

cell lines were the main factor for discrimination, proving also the robustness of PCA analysis (41).

Regarding human melanoma cells studied by Zwielly *et al.*, a distinct discrimination between the GA and GAC cells was observed after PCA analysis (38). Also, human leukemia and lymphoma cell lines investigated by Babrah *et al.* were clearly discriminated by PCA, unveiling the potential of both FTIR spectroscopy and multivariate analysis for the early detection of leukemia and lymphoma (74).

Despite these promising results, the use of cell lines as cancer models was put in doubt in a study carried out by Baker and colleagues on the prostate-derived RWPE family of cell lines (RWPE-1, RWPE-2, WPE1-NA22, WPE1-NB14, WPE1-NB11 and WPE1-NB26) (47). Non-tumorigenic cell line RWPE-1 is derived from a normal adult prostate epithelial cell transformed with a single copy of the human papillomavirus-18 and the tumorigenic cell line RWPE-2 is the result of the transformation of RWPE-1 cells with Ki-ras. Also, WPE1-NA22, WPE1-NB14, WPE1-NB11 and WPE1-NB26 cell lines were created upon the exposure of RWPE-1 to N-methyl-N-nitrosourea and exhibit increasing invasiveness (47). Using principal component – discriminant function analysis (PC-DFA), authors observed a clear discrimination of the cells. However, these results indicated that biochemical changes associated with invasiveness were not responsible for the discrimination, but rather the biochemical changes induced by different transformation methods (genetic vs. genetic and chemical) (47). Despite this, it is important to point out that FTIR spectroscopy is a suitable technique to study cancer cell lines and it is important to continue the development of new spectroscopic based applications for studying malignant cells, keeping in mind that the appropriate controls must always be used in order to be confident of the results (82). Apart from the control sample selection, it is important to define and validate all the experimental design, in particular the biological replicates and the standardization of spectral acquisition conditions. During spectroscopic data analysis, after a meticulous and exploratory direct spectra analysis, the choice of pre-treatments and the selection of the appropriate spectral region to study are of utmost importance and crucial to the success of the experiment.

1.6 Concluding remarks

Cancer cells have distinct features that separate them from normal cells. Several alterations regarding the content of lipids, proteins, nucleic acids and carbohydrates have been identified in cancer cells by FTIR spectroscopy.

Membrane lipids seem to have a stronger bonding structure in cancer cells in comparison to normal cells. Furthermore, analysis of the band at 1740 cm^{-1} can give insights on drug resistance. As for differences detected in the main protein bands (amide I and amide II), the most striking alteration is the increase of the relative amount of β-sheets in some cancer cells, which might indicate protein aggregation. Carbohydrates, particularly glycogen, are found to be decreased in cancer cells in comparison to normal cells. Furthermore, differences regarding DNA and RNA have been detected and are mainly associated with an increase of their content and a tighter packing of DNA in cancer cells.

This review highlighted the potential of FTIR spectroscopy to detect biochemical differences between distinct groups of cells. Given the fact that biochemical changes precede morphological alterations, it is likely that this technique could allow for an early diagnosis of cancer. Nevertheless, other metabolomics techniques, such as NMR and mass spectrometry, should be considered to complement results obtained by FTIR spectroscopy and discover specific metabolites that could be involved in cancer initiation and progression.

1.7 References

1. Siegel RL, Miller KD, Jemal A. Cancer statistics, 2018. CA Cancer J Clin. 2018;68(1):7–30.
2. Cancer [Internet]. WHO. 2018 [cited 2018 Feb 15]. Available from: http://www.who.int/mediacentre/factsheets/fs297/en/
3. Kendall C, Isabelle M, Bazant-Hegemark F, Hutchings J, Orr L, Babrah J, et al. Vibrational spectroscopy: a clinical tool for cancer diagnostics. Analyst. 2009;134(6):1029.
4. Machado Lopes J, Rocha-Gonçalves F, Borges M, Redondo P, Laranja-Pontes J. The cost of cancer treatment in Portugal. Ecancermedicalscience. 2017 Sep 6;11:1–10.
5. Old OJ, Fullwood LM, Scott R, Lloyd GR, Almond LM, Shepherd NA, et al. Vibrational spectroscopy for cancer diagnostics. Anal Methods. 2014;6(12):3901.
6. Lee D, Fontugne J, Gumpeni N, Park K, Macdonald TY, Robinson BD, et al. Molecular alterations in prostate cancer and association with MRI features. Prostate Cancer Prostatic Dis. 2017;20(4):430–5.
7. Denkert C, Liedtke C, Tutt A, von Minckwitz G. Molecular alterations in triple-negative breast cancer—the road to new treatment strategies. Lancet. 2017;389(10087):2430–42.
8. Cordon-Cardo C. Molecular alterations associated with bladder cancer initiation and progression. Scand J Urol Nephrol. 2008 Jan 31;42(sup218):154–65.
9. Hanahan D, Weinberg RA. Hallmarks of cancer: The next generation. Cell. 2011;144(5):646–74.
10. Pavlova NN, Thompson CB. The Emerging Hallmarks of Cancer Metabolism. Cell Metab. 2016;23(1):27–47.
11. DeBerardinis RJ, Chandel NS. Fundamentals of cancer metabolism. Sci Adv. 2016;2(5).
12. Ma Y, Zhang P, Yang Y, Wang F, Qin H. Metabolomics in the fields of oncology: a review of recent research. Mol Biol Rep. 2012 Jul 16;39(7):7505–11.
13. Serkova NJ, Glunde K. Metabolomics of Cancer. Vol. 520, Tumor Biomarker Discovery. 2009.
14. Mondul AM, Moore SC, Weinstein SJ, Männistö S, Sampson JN, Albanes D. 1-Stearoylglycerol is associated with risk of prostate cancer: results from a serum metabolomic profiling analysis. Metabolomics. 2014 Oct 7;10(5):1036–41.

15. Giskeødegård GF, Bertilsson H, Selnæs KM, Wright AJ, Bathen TF, Viset T, et al. Spermine and Citrate as Metabolic Biomarkers for Assessing Prostate Cancer Aggressiveness. Monleon D, editor. PLoS One. 2013 Apr 23;8(4):e62375.
16. Jain M, Nilsson R, Sharma S, Madhusudhan N, Kitami T, Souza AL, et al. Metabolite Profiling Identifies a Key Role for Glycine in Rapid Cancer Cell Proliferation. Science (80-). 2012 May 25;336(6084):1040–4.
17. Ellis DI, Dunn WB, Griffin JL, Allwood JW, Goodacre R. Metabolic fingerprinting as a diagnostic tool. Pharmacogenomics. 2007;8(9):1243–66.
18. Zhang A, Yan G, Han Y, Wang X. Metabolomics Approaches and Applications in Prostate Cancer Research. Appl Biochem Biotechnol. 2014 Sep 18;174(1):6–12.
19. Mackay E, Bathe OF. Cancer metabolomics and its practical applications. Glob Metab Profilling Clin Appl. 2014;70–83.
20. Kwon H, Oh S, Jin X, An YJ, Park S. Cancer metabolomics in basic science perspective. Arch Pharm Res. 2015 Mar 30;38(3):372–80.
21. Vermeersch KA, Styczynksi MP. Applications of Metabolomics in Cancer Studies. In: Journal of Carcinogenesis. 2013. p. 1–9.
22. Kaddurah-Daouk R, Kristal BS, Weinshilboum RM. Metabolomics: A Global Biochemical Approach to Drug Response and Disease. Annu Rev Pharmacol Toxicol. 2008;48(1):653–83.
23. Nassar A-EF, Talaat RE. Strategies for dealing with metabolite elucidation in drug discovery and development. Drug Discov Today. 2004 Apr;9(7):317–27.
24. Naumann D. FT-INFRARED AND FT-RAMAN SPECTROSCOPY IN BIOMEDICAL RESEARCH. Appl Spectrosc Rev. 2001 Jun 30;36(2–3):239–98.
25. Olsztynska-Janus S, Szymborska-Malek K, Gasior-Glogowska M, Walski T, Komorowska M, Witkeiwicz W, et al. Spectroscopic techniques in the study of human tissues and their components. Part I: IR spectroscopy. Acta Bioeng Biomech. 2012;14(3):101–15.
26. Singh B, Gautam R, Kumar S, Vinay Kumar BN, Nongthomba U, Nandi D, et al. Application of vibrational microspectroscopy to biology and medicine. Curr Sci. 2012;102(2):232–44.
27. Othman NH, El-tawil SG. FTIR Spectroscopy : A New Technique In Cancer Diagnoses. US Chinese J Lymphology Oncol. 2009;8(1):10–4.
28. Stuart BH. Infrared Spectroscopy Of Biological Applications: An Overview. Encycl Anal Chem. 2012;529–58.
29. Stuart BH. Infrared Spectroscopy: Fundamentals and Applications. Vol. 8, Methods.

2004. 224 p.

30. Sahu R, Mordechai S. Fourier transform infrared spectroscopy in cancer detection. Futur Oncol. 2005;1(5):635–47.
31. Sahu RK, Mordechai S. The Increasing Relevance of FTIR Spectroscopy in Biomedicine. J Med Phys Appl Sci. 2015;1(1):1–3.
32. Yano K, Sakamoto Y, Hirosawa N, Tonooka S, Katayama H, Kumaido K, et al. Applications of Fourier transform infrared spectroscopy, Fourier transform infrared microscopy and near-infrared spectroscopy to cancer research. Spectrosc Int J. 2003;17(2–3):315–21.
33. Talari ACS, Martinez MAG, Movasaghi Z, Rehman S, Rehman IU. Advances in Fourier transform infrared (FTIR) spectroscopy of biological tissues. Appl Spectrosc Rev. 2017;52(5):456–506.
34. Schmitt J, Flemming H-C. FTIR-spectroscopy in microbial and material analysis. Int Biodeterior Biodegradation. 1994;41:1–11.
35. Correia M, Lopes J, Silva R, Rosa IM, Henriques AG, Delgadillo I, et al. FTIR Spectroscopy -A Potential Tool to Identify Metabolic Changes in Dementia. HSOA J Alzheimer's Neurodegener Dis. 2016;(Building 30).
36. Gazi E, Dwyer J, Gardner P, Ghanbari-Siahkali A, Wade AP, Miyan J, et al. Applications of Fourier transform infrared microspectroscopy in studies of benign prostate and prostate cancer. A pilot study. J Pathol. 2003;201(1):99–108.
37. Liu K-Z, Xu M, Scott DA. Biomolecular characterisation of leucocytes by infrared spectroscopy. Br J Haematol. 2007;136(5):713–22.
38. Zwielly A, Gopas J, Brkic G, Mordechai S. Discrimination between drug-resistant and non-resistant human melanoma cell lines by FTIR spectroscopy. Analyst. 2009;134(2):294–300.
39. Gazi E, Baker M, Dwyer J, Lockyer NP, Gardner P, Shanks JH, et al. A Correlation of FTIR Spectra Derived from Prostate Cancer Biopsies with Gleason Grade and Tumour Stage. Eur Urol. 2006;50(4):750–61.
40. Harvey TJ, Henderson A, Gazi E, Clarke NW, Brown M, Faria EC, et al. Discrimination of prostate cancer cells by reflection mode FTIR photoacoustic spectroscopy. Analyst. 2007;132(4):292.
41. Harvey TJ, Gazi E, Henderson A, Snook RD, Clarke NW, Brown M, et al. Factors influencing the discrimination and classification of prostate cancer cell lines by FTIR microspectroscopy. Analyst. 2009;134(6):1083–91.
42. Dukor RK. Vibrational Spectroscopy in the Detection of Cancer. Handb Vib

Spectrosc. 2006;3335–60.

43. Wang L, Mizaikoff B. Application of multivariate data-analysis techniques to biomedical diagnostics based on mid-infrared spectroscopy. Anal Bioanal Chem. 2008;391(5):1641–54.
44. Magalhães S, Graça A, Tavares J, Santos MAS, Delgadillo I, Nunes A. Saccharomyces cerevisiae as a Model to Confirm the Ability of FTIR to Evaluate the Presence of Protein Aggregates. Spectr Anal Rev. 2018;6(1):1–11.
45. Worley B, Powers R. Multivariate Analysis in Metabolomics. Curr Metabolomics. 2013;1(1):92–107.
46. Sussulini A. Metabolomics : From Fundamentals to Clinical Applications. 2017. 1-351 p.
47. Baker MJ, Clarke C, Démoulin D, Nicholson JM, Lyng FM, Byrne HJ, et al. An investigation of the RWPE prostate derived family of cell lines using FTIR spectroscopy. Analyst. 2010;135(5):887–94.
48. Diem M, Boydston-White S, Chiriboga L. Infrared spectroscopy of cells and tissues: shining light onto a novel subject. Appl Spectrosc. 1999;53(4):148–61.
49. Kaur G, Dufour JM. Cell lines: Valuable tools or useless artifacts. Spermatogenesis. 2012;2(1):1–5.
50. Masters JRW. Human cancer cell lines: fact and fantasy. Nat Rev Mol Cell Biol. 2000;1(3):233–6.
51. Ulrich AB, Pour PM. Cell Lines. Encycl Genet. 2001;310–1.
52. van Staveren WCG, Solís DYW, Hébrant A, Detours V, Dumont JE, Maenhaut C. Human cancer cell lines: Experimental models for cancer cells in situ? For cancer stem cells? Biochim Biophys Acta. 2009;1795(2):92–103.
53. Gillet J-P, Varma S, Gottesman MM. The Clinical Relevance of Cancer Cell Lines. J Natl Cancer Inst. 2013;105(7):452–8.
54. Ferreira D, Adega F, Chaves R. The Importance of Cancer Cell Lines as in vitro Models in Cancer Methylome Analysis and Anticancer Drugs Testing. Oncogenomics and Cancer Proteomics - Novel Approaches in Biomarkers Discovery and Therapeutic Targets in Cancer. 2013. 139-166 p.
55. Louzada S, Adega F, Chaves R. Defining the sister rat mammary tumor cell lines HH-16 cl.2/1 and HH-16.cl.4 as an In Vitro cell model for Erbb2. PLoS One. 2012;7(1).
56. Clemens G, Hands JR, Dorling KM, Baker MJ. Vibrational spectroscopic methods for cytology and cellular research. Analyst. 2014;139(18):4411–44.

57. Rigas B, Wong PTT. Human Colon Adenocarcinoma Cell Lines Display Infrared Spectroscopic Features of Malignant Colon Tissues. Cancer Res. 1992;52(1):84–8.
58. Walsh MJ, Singh MN, Stringfellow HF, Pollock HM, Hammiche A, Grude O, et al. FTIR microspectroscopy coupled with two-class discrimination segregates markers responsible for inter- and intra-category variance in exfoliative cervical cytology. Biomark Insights. 2008;2008(3):179–89.
59. Rigas B, Morgello S, Goldman IS, Wong PT. Human colorectal cancers display abnormal Fourier-transform infrared spectra. Proc Natl Acad Sci U S A. 1990;87(20):8140–4.
60. Wong PTT, Papavassiliou ED, Rigas B. Phosphodiester Stretching Bands in the Infrared Spectra of Human Tissues and Cultured Cells. Appl Spectrosc. 1991;45(9):1563–7.
61. Barth A, Zscherp C. What vibrations tell about proteins. Q Rev Biophys. 2002;35(4):369–430.
62. Shivu B, Seshadri S, Li J, Oberg KA, Uversky VN, Fink AL. Distinct β-sheet structure in protein aggregates determined by ATR-FTIR spectroscopy. Biochemistry. 2013;52(31):5176–83.
63. Koo EH, Lansbury PT, Kelly JW. Amyloid diseases: Abnormal protein aggregation in neurodegeneration. Proc Natl Acad Sci. 1999;96(18):9989–90.
64. Levy CB, Stumbo AC, Ano Bom APD, Portari EA, Carneiro Y, Silva JL, et al. Co-localization of mutant p53 and amyloid-like protein aggregates in breast tumors. Int J Biochem Cell Biol. 2011;43(1):60–4.
65. Xu J, Reumers J, Couceiro JR, De Smet F, Gallardo R, Rudyak S, et al. Gain of function of mutant p53 by coaggregation with multiple tumor suppressors. Nat Chem Biol. 2011;7(5):285–95.
66. Yang-Hartwich Y, Bingham J, Garofalo F, Alvero AB, Mor G. Detection of p53 Protein Aggregation in Cancer Cell Lines and Tumor Samples. In: Apoptosis and Cancer: Methods and Protocols. 2015. p. 75–86.
67. Neviliappan S, Fang Kan L, Tiang Lee Walter T, Arulkumaran S, Wong PTT. Infrared spectral features of exfoliated cervical cells, cervical adenocarcinoma tissue, and an adenocarcinoma cell line (SiSo). Gynecol Oncol. 2002;85(1):170–4.
68. Bishop JM. Viral oncogenes. Vol. 42, Cell. 1985. p. 23–38.
69. Fujioka N, Morimoto Y, Arai T, Takeuchi K, Yoshioka M, Kikuchi M. Differences between infrared spectra of normal and neoplastic human gastric cells. Spectroscopy. 2004;18(1):59–66.

70. Hwang EJ, Lee SK, Kwak YH, Park SS, Hong SM. Live cells detection in breast cell-line by FTIR micro-spectrometer. In: Proceedings of IEEE Sensors. 2008. p. 878–81.
71. Mostaço-Guidolin LB, Murakami LS, Batistuti MR, Nomizo A, Bachmann L. Molecular and chemical characterization by Fourier transform infrared spectroscopy of human breast cancer cells with estrogen receptor expressed and not expressed. Spectroscopy. 2010;24(5):501–10.
72. Lee SY, Yoon KA, Jang SH, Ganbold EO, Uuriintuya D, Shin SM, et al. Infrared spectroscopy characterization of normal and lung cancer cells originated from epithelium. J Vet Sci. 2009;10(4):299–304.
73. Wong PT, Wong RK, Caputo T a, Godwin T a, Rigas B. Infrared spectroscopy of exfoliated human cervical cells: evidence of extensive structural changes during carcinogenesis. Biochemistry. 1991;88(24):10988–92.
74. Babrah J, McCarthy K, Lush RJ, Rye AD, Bessant C, Stone N. Fourier transform infrared spectroscopic studies of T-cell lymphoma, B-cell lymphoid and myeloid leukaemia cell lines. Analyst. 2009;134(4):763–8.
75. Gaigneaux A, Ruysschaert JM, Goormaghtigh E. Infrared spectroscopy as a tool for discrimination between sensitive and multiresistant K562 cells. Eur J Biochem. 2002;269(7):1968–73.
76. Le Moyec L, Tatoud R, Degeorges A, Calabresse C, Bauza G, Eugène M, et al. Proton nuclear magnetic resonance spectroscopy reveals cellular lipids involved in resistance to adriamycin and taxol by the K562 leukemia cell line. Cancer Res. 1996;56(15):3461–7.
77. Minnes R, Nissinmann M, Maizels Y, Gerlitz G, Katzir A, Raichlin Y. Using Attenuated Total Reflection–Fourier Transform Infra-Red (ATR-FTIR) spectroscopy to distinguish between melanoma cells with a different metastatic potential. Sci Rep. 2017;7(1):4381.
78. Taraboletti G, Perin L, Bottazzi B, Mantovani A, Giavazzi R, Salmona M. Membrane fluidity affects tumor-cell motility, invasion and lung-colonizing potential. Int J Cancer. 1989;44(4):707–13.
79. Parasassi T, Di Stefano M, Loiero M, Ravagnan G, Gratton E. Cholesterol modifies water concentration and dynamics in phospholipid bilayers: a fluorescence study using Laurdan probe. Biophys J. 1994;66(3):763–8.
80. Pevsner A, Diem M. Infrared Spectroscopic Studies of Major Cellular Components. Part I: The Effect of Hydration on the Spectra of Proteins. Appl Spectrosc.

2001;55(6):788–93.

81. Wood BR, Quinn MA, Burden FR, McNaughton D. An Investigation Into FTIR Spectroscopy As A Biodiagnostic Tool For Cervical Cancer. Biospectroscopy. 1996;2:143–53.
82. Erukhimovitch V, Talyshinsky M, Souprun Y, Huleihel M. Spectroscopic characterization of human and mouse primary cells, cell lines and malignant cells. Photochem Photobiol. 2002;76(4):446–51.
83. Bellisola G, Sorio C. Infrared spectroscopy and microscopy in cancer research and diagnosis. Am J Cancer Res. 2012;2(1):1–21.
84. Parker F. Applications of Infrared Spectroscopy in Biochemistry, Biology, and Medicine. 1971. 602 p.

2. Aims

This present work aimed at performing a FTIR spectroscopy study of five different prostate cell lines: PNT1A and PNT2 (derived from normal epithelial cells), 22Rv1 (derived from a primary tumor), LNCaP (derived from a lymph node metastasis) and PC-3 (derived from a bone metastasis). With this study, we intend to:

- Use FTIR spectroscopy to identify the different cell lines;
- Elucidate on biochemical differences between primary tumor and normal cells;
- Give insight on biochemical alterations that differentiate primary tumor cells from metastatic cells.

B. Results

3. Understanding prostate cancer cells metabolome: a spectroscopic approach

Francisco Santos[a,b], Sandra Magalhães[a], Magda Carvalho Henriques[b], Beatriz Silva[c], Isabel Valença[c], Daniela Ribeiro[c], Margarida Fardilha[b] and Alexandra Nunes[a]

[a] iBiMED – Institute of Biomedicine, Department of Medical Sciences, University of Aveiro, Aveiro, Portugal

[b] Signal Transduction Laboratory, iBiMED – Institute of Biomedicine, Department of Medical Sciences, University of Aveiro, Aveiro, Portugal

[c] Organelle Dynamics in Infection and Disease Laboratory, iBiMED – Institute of Biomedicine, Department of Medical Sciences, University of Aveiro, Aveiro, Portugal

Corresponding author: Alexandra Nunes, iBiMED – Institute of Biomedicine, Department of Medical Sciences, University of Aveiro, Agra do Crasto, 3810-193, Aveiro, Portugal. E-mail: alexandranunes@ua.pt

3.1 Abstract

Prostate cancer (PCa) is the second most common neoplasia in men. Because it is often diagnosed at a late stage, early diagnostic biomarkers are needed. Studying cancer metabolome, which reflects early changes that occur in cells, has gained relevance and may contribute to the identification of early diagnostic biomarkers and understanding tumor biology. Fourier-transform infrared (FTIR) spectroscopy is a metabolomics technique that probes the biochemical composition of the analyzed samples and allows to discriminate samples with distinct metabolic profiles, allowing the discrimination between cancerous and non-cancerous samples. In this study, FTIR spectra were acquired from PCa and normal prostate cell lines and analyzed by principal component analysis (PCA). Our results indicate a clear discrimination between the different cell lines, meaning that they exhibit distinct metabolic profiles. This discrimination can be attributed to an altered lipid metabolism (3000-2800 cm^{-1}, 1800-1700 cm^{-1} and 1500-1400 cm^{-1}) and the presence of protein aggregates (1622 cm^{-1}). These results suggest that studying cancer metabolome with FTIR spectroscopy not only allows the understanding of tumor pathogenesis, but also may be a valuable tool for the identification of early diagnostic biomarkers, which are crucial for a good prognosis.

3.2 Introduction

Worldwide, 1.1 million new cases of PCa were registered in 2012, 307,000 of which resulted in death. These figures place PCa as the second most common oncological disease in men, ranking just behind lung cancer (1). Many risk factors have been associated with PCa, such as race, family history and increasing age, with more than 60% of new cases being diagnosed in men aged between 60 and 70 years (1,2). Additionally, sexually transmitted infections and dietary factors are also linked to the disease (2).

One of the most conventional methods for diagnosing PCa include prostate-specific antigen (PSA) testing, which is based on its concentration in blood serum (3). High levels of PSA are often attributed to PCa. However, low levels have already been observed in PCa patients and high levels are often present in non-cancerous diseases, such as benign prostatic hyperplasia (BPH) (3,4). High levels of PSA in blood serum require a tissue biopsy, which is classified according to the Gleason grading system (5). Given the lack of specificity of the PSA test, many false positives are usually detected, resulting in a significant number of unnecessary biopsies (6). Furthermore, the Gleason grading system not always provides a consistent correlation between tissue architecture and biochemical

progression and is subject to a lack of reproducibility that arises from intra and interobserver variability (7,8). Given these drawbacks, there is a need for the development of molecular-based techniques to grade tissue samples in a reliable and reproducible manner (9,10).

An altered metabolism has been recognized as one the hallmarks of cancer (11). Metabolomics has been a valuable tool in the field of oncology, allowing the discovery of biochemical profiles and, therefore, of differences between healthy and cancer metabolic phenotypes (12). Since the metabolome reflects early changes that occur in the cell, metabolomics may allow for an early intervention because metabolic alterations are believed to precede any morphological alterations that might occur (13–15). Therefore, studying cancer metabolome not only allows the understanding of tumor pathogenesis, but also the identification of early diagnostic biomarkers, which are crucial for a good prognosis (16,17).

In recent years, FTIR spectroscopy has emerged as a tool for metabolic profiling. This approach is based on the vibrations of the atoms in a molecule caused by the interaction of infrared (IR) radiation with matter (18–20). The molecular vibrations that result from this interaction are specific to the biochemical composition of the analyzed samples and lead to spectral differences between samples, producing a fingerprint of metabolism. FTIR spectroscopy is rapid, non-invasive and reagent-free, thus it is a suitable screening technique that may allow for the discrimination between healthy and cancer samples (21–24).

Biological samples, such as cells, tissues and biofluids, are mainly composed by water. Because water has a very strong absorption in the mid-IR region, it masks the absorption of other components present in the samples, hindering FTIR analysis. Consequently, several of the experiments that have been carried out were performed on dry biological samples (25–27). FTIR spectrometers equipped with an attenuated total reflection (ATR) element can also be used to overcome the problem concerning water absorption. ATR-FTIR spectroscopy uses the total internal reflection (TIR) phenomenon. In this technique, an IR beam enters the ATR element (which can be a ZnSe, Ge or diamond ATR crystal) and undergoes TIR when the angle of incidence is greater than the critical angle. The IR beam loses energy when a material that selectively absorbs radiation is in contact with the internal reflecting element (IRE). The most important advantages of this technique include sample thickness-independent measurements and the ability to analyze live cells in

aqueous systems (28). Nonetheless, ATR-FTIR spectroscopy has also been applied to air-dried biological samples, such as cell pellets and plasma (25,26).

Regarding PCa, FTIR spectroscopy has been applied to tissue biopsies and cell lines, showing promising results and elucidating on biochemical alterations inherent to the disease (16,29–31). Cell lines present certain advantages that validate their use in preliminary studies, such as the fact that they exhibit a defined cell state that allows the analysis of a target metabolic status. Also, they evade confounding factors characteristic of biofluids and tissues (for example, age, diet and gender) (32–34). Nonetheless, cell culture suffers for not being able to replicate cell-cell and cell-matrix interactions in the tumor microenvironment, which are vital for metabolic alterations that occur with tumor progression. Therefore, models that reproduce structure, function and metabolism of in vivo tumors should be considered for further validation of in vitro studies (32,35).

The main objective of this study was to perform a FTIR spectroscopy study of three different PCa cell lines (22Rv1, LNCaP and PC-3) and two normal prostate epithelial cell lines (PNT1A and PNT2) and identify spectral differences by principal component analysis (PCA). To the best of our knowledge, this work is the first to analyze 22Rv1 and PNT1A by FTIR spectroscopy.

3.3 Material and Methods

Cell culture

Prostate cancer (22Rv1, LNCaP and PC-3) and normal prostate (PNT1A and PNT2) cell lines were cultured in RPMI-1640 culture media, supplemented with 10% FBS and 1% penicillin/streptomycin mixture, and maintained in a humidified atmosphere at 37°C containing 5% CO_2. All the reagents used in this study were purchased from Thermo Fisher Scientific. PNT2 cell line was kindly given by Dr. Ricardo Perez-Tomás (University of Barcelona, Spain), and LNCaP and PC-3 were kindly provided by Dr. Rui Medeiros (University of Porto, Portugal). 22Rv1 and PNT1A were a kind gift from Dr. Fátima Baltazar (University of Minho, Portugal). A detailed description of each cell line can be consulted in table B.1.

Table B.1: Main characteristics of the prostate cell lines.

Cell line	Derivation	Morphology	AR protein	Disease	Tumorigenic	References
PNT1A	Normal prostate epithelial cells immortalized with SV40 genome	Epithelial	Yes	Healthy	No	(79)
PNT2	Normal prostate epithelial cells immortalized with SV40 genome	Epithelial	Yes	Healthy	No	(79)
22Rv1	Primary tumor (established from xenograft CWR22R)	Epithelial	Yes	Carcinoma	Yes	(80,81)
LNCaP	Lymph node metastasis	Epithelial	Yes	Adenocarcinoma	Yes	(81,82)
PC-3	Bone metastasis	Epithelial	Yes	Adenocarcinoma	Yes	(81,83,84)

Preparation of cells

After reaching around 90% of confluency, cells were prepared for FTIR analysis. To assess viability, cells were analyzed under the microscope. The culture medium was removed from each plate and cells were detached from the plate using a solution of trypsin 0,05% and EDTA 1%. To stop the reaction, culture medium was added to the plates and the cell suspensions were transferred to separate tubes for centrifugation (3 minutes, 1000 rpm). Following centrifugation, the supernatant was discarded, and cells were resuspended in culture medium. Cells were counted using a TC20™ Automated Cell Counter, from BIO-RAD, and a total of 10^6 cells were used for each replicate (10 replicates for 22Rv1, 9 for PC-3 and 8 for LNCaP, PNT1A and PNT2). Cells were centrifuged for 3 minutes at 1000 rpm to remove the medium and resuspended in phosphate-buffered saline (PBS). Washing cells with PBS is essential to remove residual

medium and trypsin (36). PBS was removed by centrifugation (3 minutes, 1000 rpm) and cell pellets were kept on ice until FTIR analysis.

FTIR measurements

FTIR spectra were acquired in ATR mode in a FTIR spectrometer (Alpha Platinum ATR, Bruker), and processed using OPUS software (©Bruker). The spectra were obtained over the wavenumber range 4000 – 600 cm^{-1}, with a resolution of 8 cm^{-1} and 64 co-added scans. Spectra acquisition was performed in a room with controlled temperature and relative humidity (23°C and 35%, respectively). A background spectrum was acquired with the crystal empty before each different cell line and a total of 10 biological replicates for 22Rv1, 9 for PC-3 and 8 for LNCaP, PNT1A and PNT2 were used. The cell pellet was placed on the crystal and spectra were obtained after the samples were completely air-dried for, approximately, 20 minutes. Between each measurement the crystal was cleaned with ethanol 70%, followed by distilled water.

FTIR data analysis

An area peak normalization was applied to all the raw spectra, and the normalized spectra were derivatized, using the second derivative and Savitzky-Golay method. Spectra were processed using The Unscrambler X® software (v.10.4, CAMO, Oslo, Norway). The spectral regions 3000-2800 cm^{-1}, 1800-1500 cm^{-1} and 1500-900 cm^{-1} were chosen for analysis and all spectral assignments were made according to widely cited literature references.

Multivariate analysis

PCA was applied to the normalized second-derivative spectra of all the cell lines. For multivariate analysis, we used the spectral regions between 3000-2800 cm^{-1}, 1800-1500 cm^{-1} and 1500-900 cm^{-1}. All the analyses were performed on The Unscrambler X® software (v.10.4, CAMO, Oslo, Norway).

3.4 Results

Overview of FTIR spectra

Cell viability was confirmed by observation under the microscope, and each cell pellet consisted of mostly viable cells (unviable cells were discarded upon the removal of the

culture medium before trypsinization of the cells from the plate). An area peak normalization was applied to ensure that the varying cell number between replicates would not affect the spectral variances, therefore highlighting differences in biochemical structure and not in absorbance intensity (36,37).

FTIR spectral interpretation

A complete view of the averaged normalized spectra of each cell line, in the region between 4000 and 600 cm^{-1}, can be observed in figure B.1A. A direct spectral analysis of LNCaP cells has already been presented by our group (38). Briefly, in the 3000-2800 cm^{-1} region (figure B.1B), bands at 2956 and 2871 cm^{-1} are assigned to the asymmetric and symmetric stretching of CH_3 chains of lipids, respectively, whereas the bands at 2922 and 2851 cm^{-1} are attributed to the asymmetric and symmetric stretching of CH_2 chains of lipids, respectively (18,23,38,39). In the region between 1800 and 900 cm^{-1} (figure B.1C), the most prominent bands are associated with proteins: amide I (1640 cm^{-1}) and amide II (1540 cm^{-1}). The amide I band is attributed to C=O and C-N stretching of proteins, while the amide II band is assigned to N-H, C-N and C-C stretching. The amide I band is sensitive to the secondary structure of proteins and is frequently used for this type of analysis. The amide II band can also be used for studying the secondary structure of proteins, although to a lesser extent (38,40–43). Also, in this region, the band at 1740 cm^{-1} is assigned to the C=O stretching of phospholipid esters. In the 1500-900 cm^{-1} region, bands between 1480 and 1300 cm^{-1} are attributed to amino acid side chains and fatty acids and the major bands between 1300 and 900 cm^{-1} arise mainly due to carbohydrates (particularly glycogen) and phosphates associated with nucleic acids (18,23,38,39).

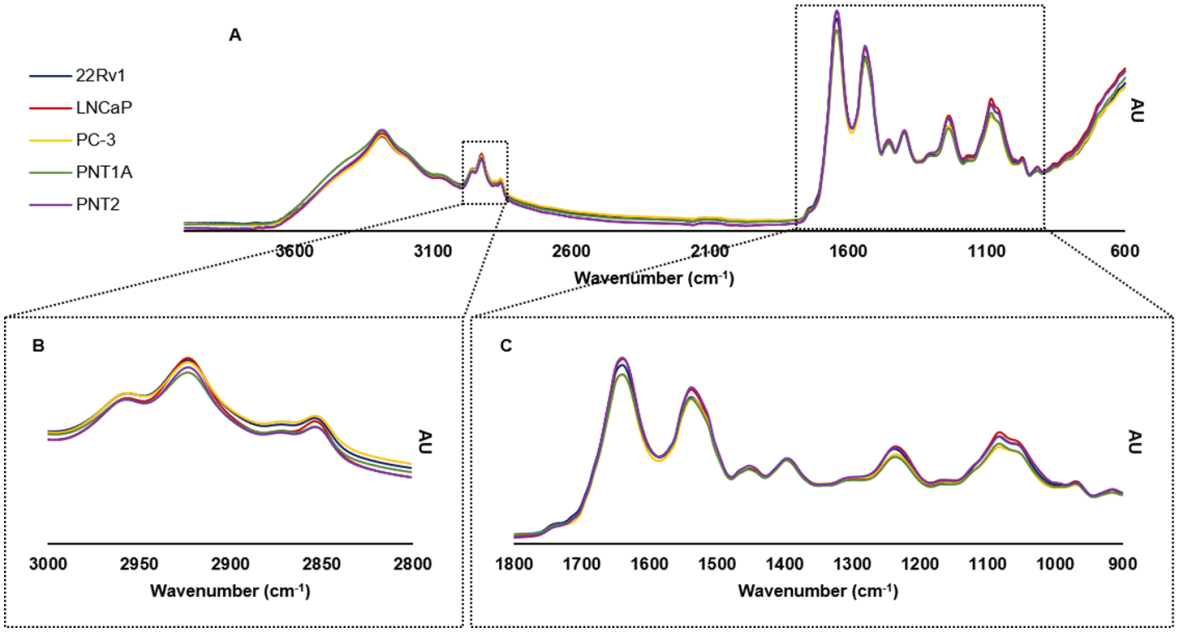

Figure B.1: Normalized mean spectra of prostate cancer (22Rv1, LNCaP and PC-3) and normal prostate (PNT1A and PNT2) cells) in the 4000-600 cm^{-1} region (A); Amplification of the regions between 3000 and 2800 cm^{-1}, and 1800 and 900 cm^{-1}. X-axis: wavenumber (cm^{-1}); Y-axis: arbitrary units (AU).

Principal Component Analysis

Before PCA analysis, spectra were normalized using an area peak algorithm and a second-order derivative using Savitzky–Golay algorithm was performed to resolve overlapping peaks and bypass variability between replicates (26,44). PCA allows to determine the most important sources of variability between prostate cancer and normal prostate cell lines. It provides score plots, which present the separation of groups observed in the samples, and loadings plots, which indicate the variables that are responsible for the discrimination (40,45). In this study, the spectral regions 3000-2800 cm^{-1}, 1800-1500 cm^{-1} and 1500-900 cm^{-1} were chosen for analysis.

Discrimination between primary tumor and normal epithelial cells

The first approach of this study was to assess whether spectra from cells of localized prostate cancer could be discriminated from those of normal prostate epithelial cells. To do so, PCA was applied to the spectra of 22Rv1 (cells derived from a primary tumor), and PNT1A and PNT2 cells (normal epithelial cells immortalized with SV40 genome).

PCA results for the 3000-2800 cm^{-1} range are presented in figure B.2. In the score plot, it is possible to observe that these cells are separated by principal component-2 (PC2), and that 22Rv1 are in negative PC2, while PNT1A and PNT2 are in positive PC2 (figure B.2A). According to the loadings plot, 22Rv1 are mainly characterized by the spectroscopic

signals located at 2917, 2874 and 2849 cm^{-1}, while PNT1A and PNT2 are characterized by the peaks at 2925 and 2857 cm^{-1} (figure B.2B).

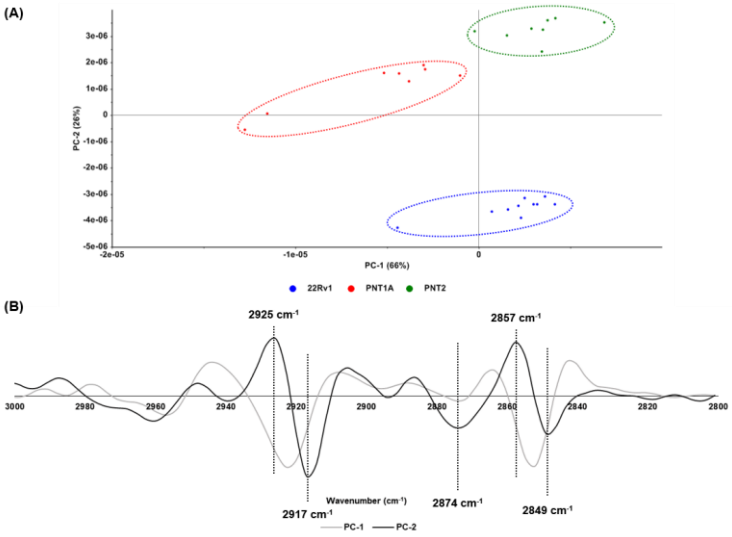

Figure B.2: PCA score (A) and loadings (B) plots from the normalized second derivative spectra of prostate cancer (22Rv1) and normal prostate (PNT1A and PNT2) cell lines on the 3000-2800 cm^{-1}.

PCA of the spectral region between 1800 and 1500 cm^{-1} is illustrated in figure B.3. In this case, the discrimination between tumor and normal cells is provided by PC3: 22Rv1 are in positive PC3, while PNT1A and PNT2 are located in negative PC3 (figure B.3A). The loadings plot indicates that the main sources of variability come from the 1700-1600 cm^{-1} region. The main spectral assignments that characterize 22Rv1 are 1679, 1665, 1648, 1622 cm^{-1}, and PNT1A and PNT2 are characterized by the peaks at 1653 and 1636 cm^{-1} (figure B.3B).

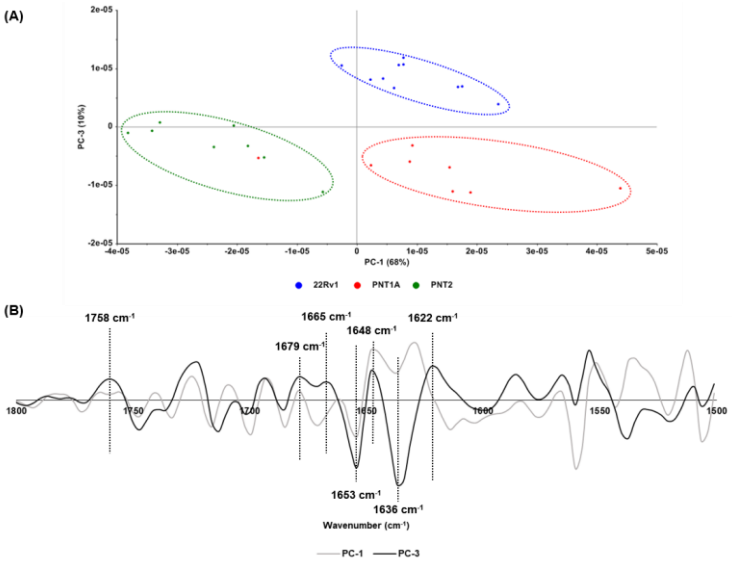

Figure B.3: PCA score (A) and loadings (B) plots from the normalized second derivative spectra of prostate cancer (22Rv1) and normal prostate (PNT1A and PNT2) cell lines on the 1800-1500 cm^{-1}.

In the 1500-900 cm^{-1} region, 22Rv1 are present in negative PC2, while PNT1A and PNT2 are located in the positive PC2 (figure B.4A). The main spectral assignments that characterize 22Rv1 are 1427, 1384, 1152, 1127, 1073, 1036, 1022 and 982 cm^{-1}. PNT1A and PNT2 are characterized by the peaks 1240, 1104, 1084, 1050 and 965 cm^{-1} (figure B.4B).

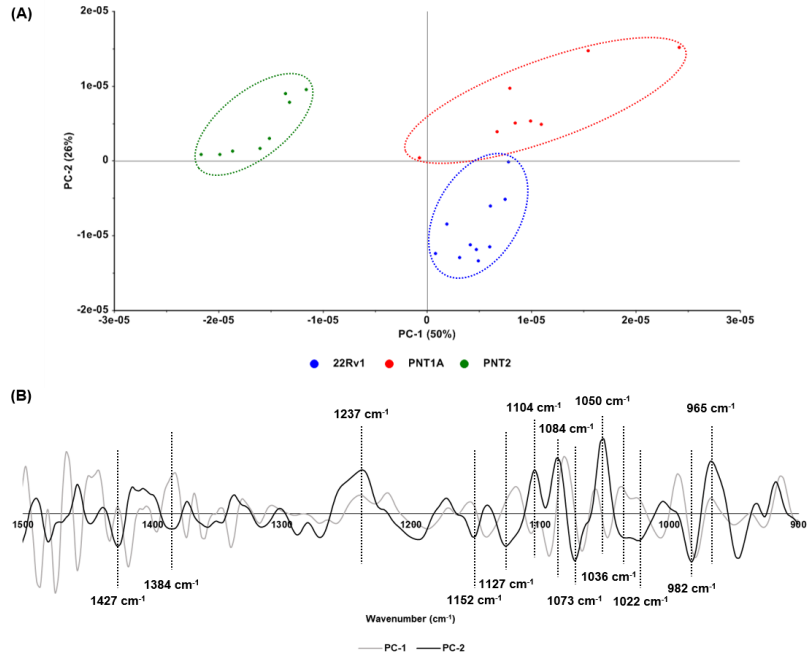

Figure B.4: PCA score (A) and loadings (B) plots from the normalized second derivative spectra of prostate cancer (22Rv1) and normal prostate (PNT1A and PNT2) cell lines on the 1500-900 cm^{-1}.

Discrimination between primary tumor and metastatic cells

To identify and classify the different prostate cancer cell lines, PCA was applied to the spectra of 22Rv1, LNCaP (derived from a lymph node metastasis) and PC-3 (derived from a bone metastasis).

PCA results for the 3000-2800 cm^{-1} region are presented in figure B.5. In the score plot, a clear discrimination of the cell lines is observed. 22Rv1 and LNCaP are located in negative PC2 and are characterized by the peaks at 2959, 2917 and 2868 cm^{-1} (figures B.5A and B.5B). PC-3 are located in positive PC2 and are characterized by the spectral assignment at 2857 cm^{-1} (figures B.5A and B.5B).

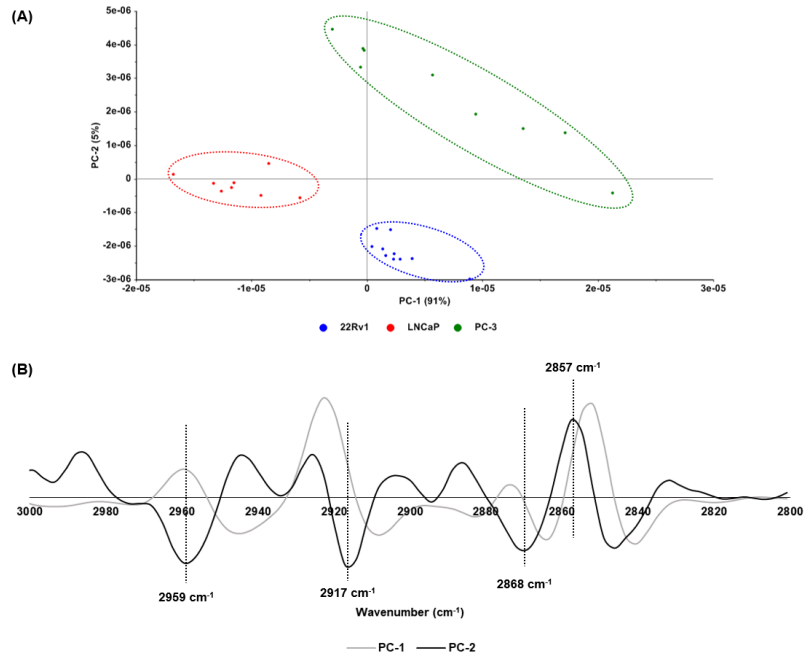

Figure B.5. PCA score (A) and loadings (B) plots from the normalized second derivative spectra of prostate cancer cell lines (22Rv1, LNCaP and PC-3) 3000-2800 cm^{-1}.

PCA for the region between 1800 and 1500 cm^{-1} is illustrated in figure B.6. A separation between 22Rv1 (negative PC2) and LNCaP and PC-3 (positive PC2) can be observed (figure B.6A). The main spectral assignments that characterize 22Rv1 are 1628, 1622 cm^{-1}, while the peaks that characterize LNCaP and PC-3 are 1747, 1651, 1636 and 1540 cm^{-1} (figure B.6B).

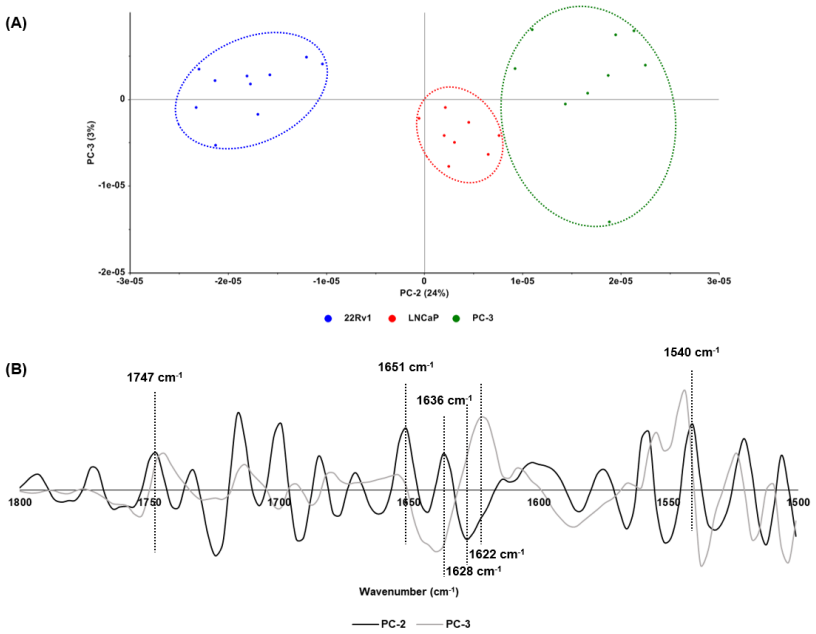

Figure B.6: PCA score (A) and loadings (B) plots from the normalized second derivative spectra of prostate cancer cell lines (22Rv1, LNCaP and PC-3) 1800-1500 cm^{-1}.

PCA results for the 1500-900 cm^{-1} region are presented in figure B.7. A distinct separation between 22Rv1 (negative PC2) and LNCaP and PC-3 (positive PC2) can be observed in the score plot (figure B.7A). The main peaks that characterize these cells are predominantly in the range between 1500 and 1400 cm^{-1} (figure B.7B).

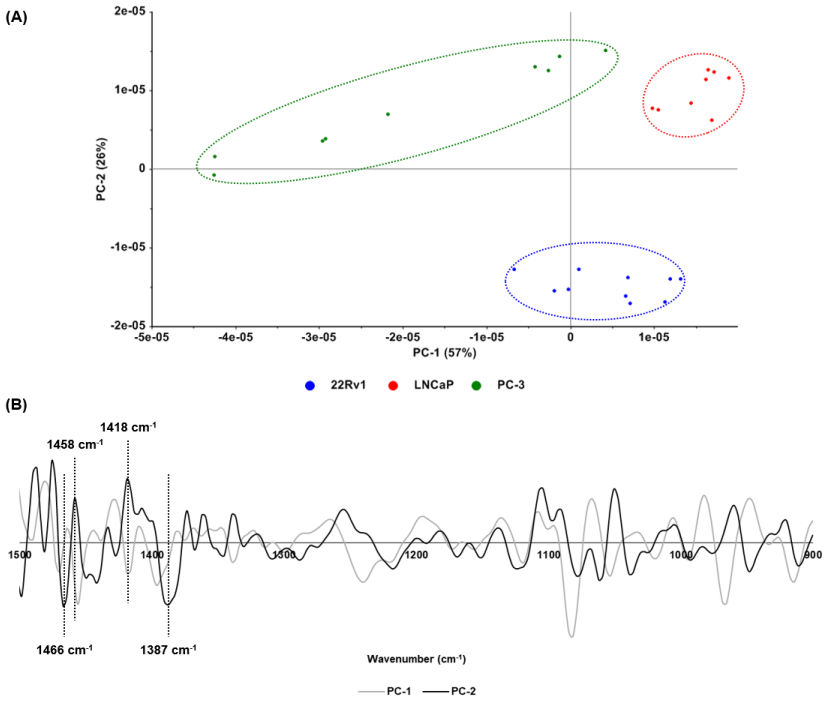

Figure B.7: PCA score (A) and loadings (B) plots from the normalized second derivative spectra of prostate cancer cell lines (22Rv1, LNCaP and PC-3) 1500-900 cm^{-1}.

3.5 Discussion

Several studies have shown the potential of FTIR spectroscopy in distinguishing the metabolic profile of normal and cancer cells. This technique has been applied to cell lines derived from numerous types of neoplasms, such as breast (42,43), cervix (44), colon (45,46), gastric (47) and lung (48) cancers.

In this study, we have demonstrated the use of FTIR spectroscopy to differentiate between prostate cell lines derived from normal epithelium (PNT1A and PNT2), primary tumor (22Rv1), and lymph node and bone metastases (LNCaP and PC-3, respectively). PCA clearly discriminated spectra from 22Rv1, and PNT1A and PNT2 in the 3000-2800 cm^{-1}, 1800-1500 cm^{-1} and 1500-900 cm^{-1} regions, indicating that they are biochemically different and, therefore, exhibit different metabolic profiles. In the spectral region from 3000 to 2800 cm^{-1}, the main spectral assignments that allowed the separation of PNT1A and PNT2 are 2925 and 2857 cm^{-1}, which arise, respectively, due to the asymmetric and

symmetric stretching vibrations of CH_2 chains of lipids. Furthermore, the bands at 2917 and 2849 cm^{-1}, which were responsible for separating 22Rv1 from PNT1A and PNT2, can also be attributed to the asymmetric and symmetric stretching vibrations of CH_2 chains of lipids. Because spectra were acquired with a resolution of 8 cm^{-1}, the aforementioned peaks can be assigned to the same biochemical component. A shift to a lower frequency might suggest alterations in the lipid composition between normal and tumor cells, and an increase in disorder of the CH_2 chains of membrane lipids have been associated with malignancy (22). Alterations in the membrane lipids have already been reported in prostate cancer tissue biopsies (30) and breast cancer-derived cell lines (42). Furthermore, alterations regarding lipid saturation have been detected in this spectral region. An increment in CH_2/CH_3 ratio suggests a change in the saturation of lipids, namely an increase of unsaturation (26). Because the main contribution to the separation observed between 22Rv1, and PNT1A and PNT2 is from CH_2 chains, we can associate these results to alterations in lipid saturation between PCa and normal cells.

In the spectral region between 1800 and 1500 cm^{-1}, the main assignments that are responsible for segregating 22Rv1 from PNT1A and PNT2 are 1758, 1679, 1665, 1648 and 1622 cm^{-1}. The peak at 1758 cm^{-1} can be attributed to the C=O stretching of lipid esters (49), suggesting a dysregulated lipid metabolism, which is known to be altered in cancer, and an accumulation of cholesterol has been reported in PCa. Also, de novo lipid synthesis has been described in PCa, which serves to produce fatty acids. Fatty acid synthesis plays an important role in cancer pathogenesis, and it is known that these newly synthesized fatty acids support cellular processes to promote cell proliferation and survival (50,51). Additionally, de novo lipogenesis has been shown to promote saturation of membrane lipids, which has consequences in terms of membrane dynamics and uptake and efficacy of chemotherapeutics (52).

The amide I band (1700-1600 cm^{-1}) arises due to the stretching vibrations of C=O and C-N, and provides information about the secondary structure of proteins, which has been extensively investigated in several studies (40,53,54). The spectral assignments specific of this region that characterize 22Rv1 are 1679, 1665, 1648 and 1622 cm^{-1}. The frequency at 1679 cm^{-1} is assigned to antiparallel β-sheets, while 1665 and 1648 cm^{-1} are related to β-turns and unordered structures, respectively (55). Regarding the peak assigned to the antiparallel β-sheets, these structures are extremely present in less soluble proteins that are likely to form aggregates (53,56). An increase in the relative amount of β-sheets, relative to α-helical segments, has already been observed in colon adenocarcinoma cell

lines (46). The peak at 1622 cm^{-1}, however, is specifically associated to the presence of protein aggregates (53,57). Cancer cells are exposed to factors that induce stress and, therefore, disrupt proteostasis, causing protein misfolding and subsequent aggregation (58). Several tumors and cancer cell lines have been found to exhibit protein aggregation, mainly involving aggregates of tumor suppressor p53 (59–61), which can play an important role in carcinogenesis (62). Also, aggregation of p53 has been associated to platinum resistance and stem cell phenotype in a subset of ovarian cancer (63), which suggests a link between loss of proteostasis and cancer progression. On the other hand, the spectral assignments that characterize PNT1A and PNT2 are 1653 and 1636 cm^{-1}, which are related to α-helices and parallel β-sheets, respectively. α-helices are usually present in more soluble proteins that are less likely to aggregate (56), and despite the presence of the assignment at 1636 cm^{-1} associated with β-sheets, this could be explained by the fact that most proteins exhibit a mixture of secondary structure (54).

A discrimination between tumor and normal cells was also observed in the spectral region between 1500 and 900 cm^{-1}. The main assignments in the 1500-1300 cm^{-1} range that characterize 22Rv1 are 1427 and 1384 cm^{-1}, the former being associated with the CH_3 and CH_2 deformation vibrations mostly due to lipid contribution, and the latter with the CH_3 symmetric wagging of phospholipids, fatty acids and triglycerides (44,64). These results may confirm the lipid alterations that were detected in other regions of the spectrum. The bands between 1460 and 1400 cm^{-1} arise due to lipid contribution, and some have been explored in previous studies. For instance, the uterine cervical adenocarcinoma cell line SiSo, along with exfoliated cervical cells and cervical adenocarcinoma tissue, exhibit an increased intensity and a shift to a lower frequency of the band at 1400 cm^{-1}, which might indicate structural changes of the CH_2 chains of lipids (44).

The bands present in the region between 1300 and 900 cm^{-1} arise mainly due to carbohydrates and phosphates associated with nucleic acids. The most important spectral assignments characteristic of 22Rv1 are 1152, 1127, 1073, 1036, 1022 cm^{-1}. The bands at 1152 and 1022 cm^{-1} are related to carbohydrates, particularly glycogen (which is specifically assigned to the frequency 1022 cm^{-1}). A reduced glycogen content has been observed in PCa tissue biopsies (30), and cervical adenocarcinoma tissue and cervical adenocarcinoma cells (44). The decrease in glycogen content in malignant cells can be attributed to their higher metabolic activity and, thus, an increase in glycolysis (16,22,44,65). The remaining bands (1127, 1073 and 1036 cm^{-1}) account for differences associated with nucleic acids. This could be linked to the fact that nucleic acids exhibit

increased hydrogen-bonding of the phosphodiester groups and a higher level of packing in cancer cells, as confirmed by several studies (46).

The second part of this study consisted in discriminating primary tumor cells from cells derived from lymph node and bone metastases. To do so, we applied PCA to the spectra of 22Rv1 and to those of LNCaP (derived from lymph node metastasis) and PC-3 (derived from bone metastasis). The PCA results indicate that the three cancer cell lines exhibit distinct metabolic profiles, as they are clearly separated in the three spectral regions that were analyzed. It is already known that metastatic cells exhibit different metabolic profiles as they colonize different organs (66).

In the spectral region between 3000 and 2800 cm^{-1}, the cells appeared to be well separated from each other. LNCaP and 22Rv1 are characterized by the same assignments (2959, 2917 and 2868 cm^{-1}), suggesting that they are somewhat similar in terms of lipid constitution. On the other hand, the peak that characterizes PC-3 cells is 2857 cm^{-1}. Like the results obtained comparing primary tumor with normal cells, these results also suggest that 22Rv1 and LNCaP exhibit differences in the methylene chains of lipids in comparison to PC-3. In the 1800-1700 cm^{-1} region, however, LNCaP and PC-3 are grouped in the same PC and are characterized by the peak at 1747 cm^{-1} (associated with lipids and fatty acids). Metabolic reprogramming is essential for cancer cells to escape from a primary tumor, overcome nutrient and energy deficit, survive and, subsequently, form metastases. However, the role of lipid metabolism that confers the aggressive properties of malignant cancers is still unknown (67). Nonetheless, exchanges of fatty acids between adipocytes and PC-3 cells have been observed by FTIR spectroscopy (68), and this process is considered an adaptive metabolic process set up by cancer cells to take full advantage of the lipids stored in cells present in the tumor microenvironment. Also, certain subclasses of lipids, such as phosphatidylcholines, phosphatidylethanolamines and glycerophosphoinositols, have been found to be present in higher levels in PCa cells derived from distant metastatic sites, including LNCaP and MDAPCa2b (derived from a bone metastasis) (69), indicating active membrane remodeling and cellular proliferation (70).

Some remarkable differences were also detected in the amide I region. The peak associated with protein aggregation (1622 cm^{-1}) was partly responsible for segregating 22Rv1 from LNCaP and PC-3. Furthermore, the spectral assignment at 1628 cm^{-1} also characterized 22Rv1 cells. This peak can be attributed to the presence of β-sheets (40,55). However, the peaks that characterize LNCaP and PC-3 (1651 and 1636 cm^{-1}) do

not suggest the presence of protein aggregates in these cells but might indicate a change in the protein secondary structure. Regarding the amide II band (1600-1500 cm^{-1}), the peak at 1540 cm^{-1} also seems to be partly responsible for discriminating LNCaP and PC-3 from 22Rv1. It has been reported that cells with higher metastatic potential exhibit a higher absorption intensity of the amide II band (28). The high level of fluidity of the cell membrane that metastatic cells exhibit can be associated with an increase in the level of hydration, which is followed by an increment in the absorption intensity of proteins (71–73). Some variability also seems to come from the spectral range between 1500 and 1400 cm^{-1}, which arises due to lipid contribution, confirming that the lipids play an important role in discriminating primary tumor and metastatic cells.

In this study, FTIR spectroscopy and PCA were successfully applied to three PCa (22Rv1, LNCaP and PC-3) and two normal prostate (PNT1A and PNT2) cell lines. Our results clearly indicate that this technique, coupled with multivariate analysis, can be used to distinguish the different types of prostate cells in several spectral regions. However, in order to validate our results, other biological samples should be considered for analysis, such as human urine, serum/plasma and prostatic fluid (74). Also, because FTIR spectroscopy is uncapable of detecting specific metabolites that are responsible for causing changes, other metabolomic techniques should be considered, such as mass spectrometry and nuclear magnetic resonance. Prostate cancer metabolome has been studied by these techniques, allowing the identification of metabolites implicated in certain metabolic pathways (75–78). Nevertheless, our results indicate that primary tumor cells can be distinguished from normal cells, and that the former differ from metastatic cells. Lipid metabolism obviously plays an important role in tumorigenesis and metastasis, and other alterations, such as protein aggregation, can also be an important event in cancer progression. Given the fact that the biochemical composition of the prostate cell lines can be detected by FTIR, it could be useful in providing an early diagnosis and understanding tumor biology.

3.6 References

1. Ferlay J, Soerjomataram I, Dikshit R, Eser S, Mathers C, Rebelo M, et al. Cancer incidence and mortality worldwide: Sources, methods and major patterns in GLOBOCAN 2012. Int J Cancer. 2015;136(5):E359–86.
2. Nelson WG, De Marzo AM, Isaacs WB. Prostate Cancer. N Engl J Med. 2003;349(4):366–81.
3. Kellokumpu-Lehtinen P, Nurmi M, Koskinen P, Irjala K. Prostate-specific antigen as a marker of adenocarcinoma of prostate. Urol Res. 1989;17(4):245–9.
4. Thompson IM, Pauler DK, Goodman PJ, Tangen CM, Scott LM, Parnes HL, et al. Prevalence of Prostate Cancer among Men with a Prostate-Specific Antigen Level ≤4.0 ng per Milliliter. N Engl J Med. 2004;350(22):2239–46.
5. Gleason DF. Histologic grading and clinical staging of prostatic carcinom. Urol Pathol prostate , M Tann Ed Philadelphia, PA Lea Febiger. 1977;171–97.
6. Bhargava R. Towards a practical Fourier transform infrared chemical imaging protocol for cancer histopathology. Anal Bioanal Chem. 2007;389(4):1155–69.
7. Têtu B. Morphologic changes induced by neoadjuvant combination hormone therapy on prostatic tissue and prostate cancer. Endocr Relat Cancer. 1996;3(3):165–70.
8. Lattouf JB, Saad F. Gleason score on biopsy: Is it reliable for predicting the final grade on pathology? BJU Int. 2002;90(7):694–8.
9. Levin IW, Bhargava R. FOURIER TRANSFORM INFRARED VIBRATIONAL SPECTROSCOPIC IMAGING: Integrating Microscopy and Molecular Recognition. Annu Rev Phys Chem. 2005;56(1):429–74.
10. Mackanos MA, Contag CH. FTIR microspectroscopy for improved prostate cancer diagnosis. Trends Biotechnol. 2009;27(12):661–3.
11. Hanahan D, Weinberg RA. Hallmarks of cancer: The next generation. Cell. 2011;144(5):646–74.
12. Aboud OA, Weiss RH. New opportunities from the cancer metabolome. Clin Chem. 2013;59(1):138–46.
13. Zhang A, Yan G, Han Y, Wang X. Metabolomics Approaches and Applications in Prostate Cancer Research. Appl Biochem Biotechnol. 2014 Sep 18;174(1):6–12.
14. Vermeersch KA, Styczynksi MP. Applications of Metabolomics in Cancer Studies. J Carcinog. 2013;12(9):1–9.
15. Roberts MJ, Schirra HJ, Lavin MF, Gardiner RA. Metabolomics: A novel approach to early and noninvasive prostate cancer detection. Korean J Urol. 2011;52(2):79–

89.

16. Gazi E, Dwyer J, Gardner P, Ghanbari-Siahkali A, Wade AP, Miyan J, et al. Applications of Fourier transform infrared microspectroscopy in studies of benign prostate and prostate cancer. A pilot study. J Pathol. 2003;201(1):99–108.
17. Eidelman E, Twum-Ampofo J, Ansari J, Siddiqui MM. The Metabolic Phenotype of Prostate Cancer. Front Oncol. 2017;7:1–6.
18. Ellis DI, Dunn WB, Griffin JL, Allwood JW, Goodacre R. Metabolic fingerprinting as a diagnostic tool. Pharmacogenomics. 2007;8(9):1243–66.
19. Olsztynska-Janus S, Szymborska-Malek K, Gasior-Glogowska M, Walski T, Komorowska M, Witkeiwicz W, et al. Spectroscopic techniques in the study of human tissues and their components. Part I: IR spectroscopy. Acta Bioeng Biomech. 2012;14(3):101–15.
20. Stuart BH. Infrared Spectroscopy Of Biological Applications: An Overview. Encycl Anal Chem. 2012;529–58.
21. Kendall C, Isabelle M, Bazant-Hegemark F, Hutchings J, Orr L, Babrah J, et al. Vibrational spectroscopy: a clinical tool for cancer diagnostics. Analyst. 2009;134(6):1029.
22. Othman NH, El-tawil SG. FTIR Spectroscopy : A New Technique In Cancer Diagnoses. US Chinese J Lymphology Oncol. 2009;8(1):10–4.
23. Stuart BH. Infrared Spectroscopy: Fundamentals and Applications. Vol. 8, Methods. 2004. 224 p.
24. Griffin JL, Shockcor JP. Metabolic profiles of cancer cells. Nat Rev Cancer. 2004;4(7):551–61.
25. Correia M, Lopes J, Silva R, Rosa IM, Henriques AG, Delgadillo I, et al. FTIR Spectroscopy -A Potential Tool to Identify Metabolic Changes in Dementia. HSOA J Alzheimer's Neurodegener Dis. 2016;2(7):1–9.
26. Denbigh JL, Perez-Guaita D, Vernooij RR, Tobin MJ, Bambery KR, Xu Y, et al. Probing the action of a novel anti-leukaemic drug therapy at the single cell level using modern vibrational spectroscopy techniques. Sci Rep. 2017;7(1):1–12.
27. Schmitt J, Flemming H-C. FTIR-spectroscopy in microbial and material analysis. Int Biodeterior Biodegradation. 1994;41:1–11.
28. Minnes R, Nissinmann M, Maizels Y, Gerlitz G, Katzir A, Raichlin Y. Using Attenuated Total Reflection–Fourier Transform Infra-Red (ATR-FTIR) spectroscopy to distinguish between melanoma cells with a different metastatic potential. Sci Rep. 2017;7(1):4381.

29. Harvey TJ, Gazi E, Henderson A, Snook RD, Clarke NW, Brown M, et al. Factors influencing the discrimination and classification of prostate cancer cell lines by FTIR microspectroscopy. Analyst. 2009;134(6):1083–91.
30. Felgueiras J, Vieira Silva J, Nunes A, Patrício A, Pelech S, Fardilha M. Understanding prostate cancer biology using metabolomics and proteomics approaches: potentials in the improvement of the diagnosis, prognosis and identification of new therapeutic targets. Eur J Cancer. 2017;72(January):S192.
31. Harvey TJ, Henderson A, Gazi E, Clarke NW, Brown M, Faria EC, et al. Discrimination of prostate cancer cells by reflection mode FTIR photoacoustic spectroscopy. Analyst. 2007;132(4):292.
32. Halama A. Metabolomics in cell culture - A strategy to study crucial metabolic pathways in cancer development and the response to treatment. Arch Biochem Biophys. 2014;564:100–9.
33. Zhang A, Sun H, Xu H, Qiu S, Wang X. Cell Metabolomics. Omi A J Integr Biol. 2013;17(10):495–501.
34. Čuperlović-Culf M, Barnett DA, Culf AS, Chute I. Cell culture metabolomics: Applications and future directions. Drug Discov Today. 2010;15(15–16):610–21.
35. Keshari KR, Sriram R, Criekinge M Van, Wilson DM, Zhen J, Vigneron DB, et al. Metabolic Reprogramming and Validation of Hyperpolarized 13C Lactate as a Prostate Cancer Biomarker Using a Human Prostate Tissue Slice Culture Bioreactor. 2014;73(11):1171–81.
36. Baker MJ, Trevisan J, Bassan P, Bhargava R, Butler HJ, Dorling KM, et al. Using Fourier transform IR spectroscopy to analyze biological materials. Nat Protoc. 2014;9(8):1771–91.
37. Mostaço-Guidolin LB, Murakami LS, Batistuti MR, Nomizo A, Bachmann L. Molecular and chemical characterization by Fourier transform infrared spectroscopy of human breast cancer cells with estrogen receptor expressed and not expressed. Spectroscopy. 2010;24(5):501–10.
38. Santos F, Magalhães S, Henriques MC, Fardilha M, Nunes A. Spectroscopic features of cancer cells: FTIR spectroscopy as a tool for early diagnosis. Curr Metabolomics. 2018;6(2):103-11.
39. Naumann D. FT-INFRARED AND FT-RAMAN SPECTROSCOPY IN BIOMEDICAL RESEARCH. Appl Spectrosc Rev. 2001 Jun 30;36(2–3):239–98.
40. Magalhães S, Graça A, Tavares J, Santos MAS, Delgadillo I, Nunes A. Saccharomyces cerevisiae as a Model to Confirm the Ability of FTIR to Evaluate

the Presence of Protein Aggregates. Spectr Anal Rev. 2018;6(1):1–11.

41. Shivu B, Seshadri S, Li J, Oberg KA, Uversky VN, Fink AL. Distinct β-sheet structure in protein aggregates determined by ATR-FTIR spectroscopy. Biochemistry. 2013;52(31):5176–83.
42. Miller LM, Bourassa MW, Smith RJ. FTIR spectroscopic imaging of protein aggregation in living cells. Biochim Biophys Acta. 2013;1828(10):2339–46.
43. Barth A, Zscherp C. What vibrations tell about proteins. Q Rev Biophys. 2002;35(4):369–430.
44. Ricciardi V, Portaccio M, Piccolella S, Manti L, Pacifico S, Lepore M. Study of SH-SY5Y cancer cell response to treatment with polyphenol extracts using FT-IR spectroscopy. Biosensors. 2017;7(4):1–16.
45. Sussulini A. Metabolomics : From Fundamentals to Clinical Applications. 2017. 1-351 p.
46. Hwang EJ, Lee SK, Kwak YH, Park SS, Hong SM. Live cells detection in breast cell-line by FTIR micro-spectrometer. In: Proceedings of IEEE Sensors. 2008. p. 878–81.
47. Neviliappan S, Fang Kan L, Tiang Lee Walter T, Arulkumaran S, Wong PTT. Infrared spectral features of exfoliated cervical cells, cervical adenocarcinoma tissue, and an adenocarcinoma cell line (SiSo). Gynecol Oncol. 2002;85(1):170–4.
48. Rigas B, Morgello S, Goldman IS, Wong PT. Human colorectal cancers display abnormal Fourier-transform infrared spectra. Proc Natl Acad Sci U S A. 1990;87(20):8140–4.
49. Rigas B, Wong PTT. Human Colon Adenocarcinoma Cell Lines Display Infrared Spectroscopic Features of Malignant Colon Tissues. Cancer Res. 1992;52(1):84–8.
50. Fujioka N, Morimoto Y, Arai T, Takeuchi K, Yoshioka M, Kikuchi M. Differences between infrared spectra of normal and neoplastic human gastric cells. Spectroscopy. 2004;18(1):59–66.
51. Lee SY, Yoon KA, Jang SH, Ganbold EO, Uuriintuya D, Shin SM, et al. Infrared spectroscopy characterization of normal and lung cancer cells originated from epithelium. J Vet Sci. 2009;10(4):299–304.
52. Wehbe K, Pineau R, Eimer S, Vital A, Loiseau H, Déléris G. Differentiation between normal and tumor vasculature of animal and human glioma by FTIR imaging. Analyst. 2010;135(12):3052–9.
53. Griffin JE. Androgen Resistance - The Clinical and Molecular Spectrum. N Engl J Med. 1992;326(9):611–8.

54. Menendez JA, Lupu R. Fatty acid synthase and the lipogenic phenotype in cancer pathogenesis. Nat Rev Cancer. 2007;7(10):763–77.
55. Rysman E, Brusselmans K, Scheys K, Timmermans L, Derua R, Munck S, et al. De novo lipogenesis protects cancer cells from free radicals and chemotherapeutics by promoting membrane lipid saturation. Cancer Res. 2010;70(20):8117–26.
56. Talari ACS, Martinez MAG, Movasaghi Z, Rehman S, Rehman IU. Advances in Fourier transform infrared (FTIR) spectroscopy of biological tissues. Appl Spectrosc Rev. 2017;52(5):456–506.
57. Kumar S, Srinivasan A, Nikolajeff F. Role of infrared spectroscopy and imaging in cancer diagnosis. Curr Med Chem. 2017;24(May).
58. Hetz C, Chevet E, Oakes SA. Proteostasis control by the unfolded protein response. Nat Cell Biol. 2015;17(7):829–38.
59. Koo EH, Lansbury PT, Kelly JW. Amyloid diseases: Abnormal protein aggregation in neurodegeneration. Proc Natl Acad Sci. 1999;96(18):9989–90.
60. Levy CB, Stumbo AC, Ano Bom APD, Portari EA, Carneiro Y, Silva JL, et al. Co-localization of mutant p53 and amyloid-like protein aggregates in breast tumors. Int J Biochem Cell Biol. 2011;43(1):60–4.
61. Xu J, Reumers J, Couceiro JR, De Smet F, Gallardo R, Rudyak S, et al. Gain of function of mutant p53 by coaggregation with multiple tumor suppressors. Nat Chem Biol. 2011;7(5):285–95.
62. Yang-Hartwich Y, Bingham J, Garofalo F, Alvero AB, Mor G. Detection of p53 Protein Aggregation in Cancer Cell Lines and Tumor Samples. In: Apoptosis and Cancer: Methods and Protocols. 2015. p. 75–86.
63. Yang-Hartwich Y, Soteras MG, Lin ZP, Holmberg J, Sumi N, Craveiro V, et al. P53 Protein Aggregation Promotes Platinum Resistance in Ovarian Cancer. Oncogene. 2014;34(27):3605–16.
64. Bellisola G, Sorio C. Infrared spectroscopy and microscopy in cancer research and diagnosis. Am J Cancer Res. 2012;2(1):1–21.
65. Clemens G, Hands JR, Dorling KM, Baker MJ. Vibrational spectroscopic methods for cytology and cellular research. Analyst. 2014;139(18):4411–44.
66. Pascual G, Dom D. The contributions of cancer cell metabolism to metastasis. 2018;
67. Luo X, Cheng C, Tan Z, Li N, Tang M, Yang L, et al. Emerging roles of lipid metabolism in cancer metastasis. Mol Cancer. 2017;16(1):1–10.
68. Gazi E, Gardner P, Lockyer NP, Hart CA, Brown MD, Clarke NW. Direct evidence

of lipid translocation between adipocytes and prostate cancer cells with imaging FTIR microspectroscopy. J Lipid Res. 2007;48(8):1846–56.

69. Burch TC, Isaac G, Booher CL, Rhim JS, Rainville P, Langridge J, et al. Comparative metabolomic and lipidomic analysis of phenotype stratified prostate cells. PLoS One. 2015;10(8):1–16.
70. Swanson MG, Keshari KR, Tabatabai ZL, Simko JP, Shinohara K, Carroll PR, et al. Quantification of choline- and ethanolamine-containing metabolites in human prostate tissues using 1H HR-MAS total correlation spectroscopy. Magn Reson Med. 2008;60(1):33–40.
71. Taraboletti G, Perin L, Bottazzi B, Mantovani A, Giavazzi R, Salmona M. Membrane fluidity affects tumor-cell motility, invasion and lung-colonizing potential. Int J Cancer. 1989;44(4):707–13.
72. Parasassi T, Di Stefano M, Loiero M, Ravagnan G, Gratton E. Cholesterol modifies water concentration and dynamics in phospholipid bilayers: a fluorescence study using Laurdan probe. Biophys J. 1994;66(3):763–8.
73. Pevsner A, Diem M. Infrared Spectroscopic Studies of Major Cellular Components. Part I: The Effect of Hydration on the Spectra of Proteins. Appl Spectrosc. 2001;55(6):788–93.
74. Lima AR, Bastos M de L, Carvalho M, Guedes de Pinho P. Biomarker discovery in human prostate cancer: An update in metabolomics studies. Transl Oncol. 2016;9(4):357–70.
75. Mondul AM, Moore SC, Weinstein SJ, Männistö S, Sampson JN, Albanes D. 1-Stearoylglycerol is associated with risk of prostate cancer: results from a serum metabolomic profiling analysis. Metabolomics. 2014 Oct 7;10(5):1036–41.
76. Giskeødegård GF, Bertilsson H, Selnæs KM, Wright AJ, Bathen TF, Viset T, et al. Spermine and Citrate as Metabolic Biomarkers for Assessing Prostate Cancer Aggressiveness. Monleon D, editor. PLoS One. 2013 Apr 23;8(4):e62375.
77. Khan AP, Rajendiran TM, Bushra A, Asangani IA, Athanikar JN, Yocum AK, et al. The Role of Sarcosine Metabolism in Prostate Cancer Progression. Neoplasia. 2013;15(5):491-IN13.
78. Sreekumar A, Poisson LM, Rajendiran TM, Khan AP, Cao Q, Yu J, et al. Metabolomic profiles delineate potential role for sarcosine in prostate cancer progression. Nature. 2009;457(7231):910–4.
79. Berthon P, Cussenot O, Hopwood L, Le Duc A, Maitland NJ. Functional expression of SV40 in normal human prostatic epithelial and fibroblastic cells: Differentiation

pattern of non-tumorigenic cell lines. Int J Oncol. 1995;6(2):333–43.

80. Sramkoski RM, Pretlow TG, Giaconia JM, Pretlow TP, Schwartz S, Sy MS, et al. A new human prostate carcinoma cell line, 22Rv1. In Vitro Cell Dev Biol Anim. 1999;35(August):403–9.
81. van Bokhoven A, Varella-Garcia M, Korch C, Johannes WU, Smith EE, Miller HL, et al. Molecular characterization of human prostate carcinoma cell lines. Prostate. 2003;57(3):205–25.
82. Horoszewicz JS, Leong SS, Kawinski E, Karr JP, Rosenthal H, Chu TM, et al. LNCaP Model of Human Prostatic Carcinoma. Cancer Res. 1983;43(4):1809–18.
83. Alimirah F, Chen J, Basrawala Z, Xin H, Choubey D. DU-145 and PC-3 human prostate cancer cell lines express androgen receptor: Implications for the androgen receptor functions and regulation. FEBS Lett. 2006;580(9):2294–300.
84. Kaighn ME, Narayan KS, Ohnuki Y, Lechner JF, Jones LW. Establishment and characterization of a human prostatic carcinoma cell line (PC-3). Invest Urol. 1979;17(1):16–23.

C. Concluding remarks, limitations and future perspectives

4. Concluding remarks

The main goal of this dissertation was to apply FTIR spectroscopy to PCa and normal prostate cell lines. Principal component analysis allowed us to identify spectral differences between the cells, and our results indicate that:

- 22Rv1 were characterized by spectral assignments associated with CH_2 chains of lipids (2917 and 2849 cm^{-1}), suggesting that these cells, in comparison with normal epithelial cells, exhibit structural alterations in membrane lipids;
- Lipid metabolism plays an important role in tumorigenesis, which is evidenced by the spectral assignments 1758, 1427 and 1384 cm^{-1};
- Protein aggregation (1622 cm^{-1}), which may result from loss of proteostasis, may be an important event during cancer progression.
- Metastatic cells (LNCaP and PC-3) are mainly characterized by the spectral assignments 1747, 1458 and 1418 cm^{-1}, suggesting that these cells exhibit differences in their lipid metabolism in comparison to primary tumor cells.

Overall, these results indicate that FTIR spectroscopy was able to detect the biochemical composition of the studied cell lines, indicating that they exhibit different metabolic profiles. Thus, this technique could be useful in providing an early diagnosis and understanding tumor biology.

5. Limitations and future perspectives

Despite the promising results and the potentiality of FTIR spectroscopy in studying cancer cell lines, a few restrictions of this study should be considered. Although cell culture is the most useful *in vitro* model for studying PCa, it does not account for metabolic alterations that result from cell-cell and cell-matrix interactions. Therefore, important alterations might not have been detected in this study. However, apart from the work presented in this dissertation, FTIR spectroscopy has also been applied to human prostate tissues by our group. Nevertheless, further investigation using other biological samples should be carried out. Because prostatic fluid reflects prostate physiology, it seems like a suitable candidate for future studies involving metabolic profiling with FTIR spectroscopy.

Additionally, in spite of providing a general view of a cell's metabolism, FTIR spectroscopy is not able to identify specific metabolites that might be involved in important metabolic processes. Therefore, other techniques (mass spectrometry and nuclear magnetic resonance, for instance) should be considered for a more detailed analysis of PCa metabolome.